powders

MDPI

Article

Selective Separation of SiO_2 and SnO_2 Particles in the Submicron Range: Investigating Salt and Surfactant Adsorption Parameter

Claudia Heilmann [1,*], Lisa Ditscherlein [1], Martin Rudolph [2] and Urs Alexander Peuker [1,*]

[1] Institute of Mechanical Process Engineering and Mineral Processing, TU Bergakademie Freiberg, 09599 Freiberg, Germany; lisa.ditscherlein@mvtat.tu-freiberg.de
[2] Helmholtz-Zentrum Dresden-Rossendorf, Helmholtz Institute Freiberg for Ressource Technology, 09599 Freiberg, Germany; m.rudolph@hzdr.de
* Correspondence: claudia.heilmann@extern.tu-freiberg.de (C.H.); urs.peuker@mvtat.tu-freiberg.de (U.A.P.)

Abstract

The separation of particles smaller than 1 µm either by composition or by size is still a challenge. For the separation of SiO_2 and SnO_2, the creation of a selective separation feature and the specific adsorption of salts and surfactants were investigated. The adsorption of various salts, e.g., $AlCl_3$, $ZnCl_2$, $MnCl_2$ and $MgCl_2$ were therefore analyzed, and the necessary concentration for the charge reversal of the material was determined. It was noticed that the investigated materials differ in their isoelectric point (IEP) and therefore in their adsorption behavior because only $ZnCl_2$ and $MgCl_2$ are suitable for a charge reversal of both metal oxides. The phase transfer of the pure material at different pH values with $ZnCl_2$ or $MgCl_2$ and sodium dodecyl sulfate (SDS) revealed that the adsorption behavior of the particle has an influence on the phase transfer. As a result, the phase transfer of SiO_2 is pH dependent, whereas the phase transfer of SnO_2 operates over a wider pH range. This allowed the separation of SiO_2 and SnO_2 to be controlled by the salt and surfactant concentration as well as pH. The separation of SiO_2 and SnO_2 was investigated for various parameters such as salt and surfactant concentration, particle concentration and composition of the mixture. Also, pH 8, where a selective phase transfer for SiO_2 occurs, and pH 6, where the greatest difference between the materials exists, were also investigated. By comparing the parameters, it was found that the combination of $ZnCl_2$/SDS and $MgCl_2$/SDS enables a selective separation of the materials. Furthermore, it was also found that the concentration of SDS has a significant effect on the separation, as the formation of a bilayer structure is important for the separation, and therefore, higher SDS concentrations are required at higher particle concentrations to increase the separation efficiency.

Keywords: separation; interface; adsorption; submicron range; SDS; XRF

check for updates

Academic Editor: Chunfeng Hu

Received: 15 February 2025
Revised: 15 April 2025
Accepted: 30 April 2025
Published: 3 July 2025

Citation: Heilmann, C.; Ditscherlein, L.; Rudolph, M.; Peuker, U.A. Selective Separation of SiO_2 and SnO_2 Particles in the Submicron Range: Investigating Salt and Surfactant Adsorption Parameter. *Powders* **2025**, *4*, 19. https://doi.org/10.3390/powders4030019

Copyright: © 2025 by the authors. Licensee MDPI, Basel, Switzerland. This article is an open access article distributed under the terms and conditions of the Creative Commons Attribution (CC BY) license (https://creativecommons.org/licenses/by/4.0/).

1. Introduction

To separate particles, various physical or chemical separation methods can be used [1]. The various separation methods address different properties, such as density [2], size [3–5], wetting properties [3] or magnetic properties [6]. The possibility of separating ultrafine or submicron particles is very limited, as the selectivity of many separation methods fails at these sizes [3,5,7]. For example, in separation processes where the density properties of the materials are addressed, the separation loses its selectivity at sizes below 30 µm to 10 µm [7], since drag effects become dominant compared to inertia effects. As the

particle size decreases, the selectivity-generating forces become less effective compared to the contribution of the flow field of the surrounding medium and the particles follow the streamlines as a collective. This prevents any separation effects, e.g., by size, shape or composition. For this reason, several new approaches, which are able to overcome the problem, have recently been investigated to separate particles smaller than 10 µm; for example, the minimum of floatability is reached at a particle size in the lower micrometer range between 3 µm and 5 µm [3,5,8,9]. Nanoparticles can also be transferred from one phase to the other in a centrifugal field. However, it was noted that the sedimentation of the particles during centrifugation prevents the transfer to the organic phase [10]. For a liquid–liquid extraction, it is also possible to transfer particles in the nanoparticle range to the other phase [10–14]. In order to separate particles with this process, the particles would have to differ greatly in their wetting properties.

In flotation and liquid–liquid extraction, particle separation is bases on physical and chemical surface properties [1,15–17]. In both cases, only hydrophobic particles can attach to the gas bubble or oil droplet and thus be separated, while hydrophilic particles remain in the aqueous phase [1,18].

In order to hydrophobize particles, amphiphilic molecules, i.e., surfactants, are used to adsorb to the particle surface, which are known as collectors. As the surfactants do not adsorb to a specific surface [19,20], the activation of the particle surface is needed [21,22]. For example, various salts containing Ca^{2+}, Mg^{2+} or Pb^{2+} ions are used as activators in the collector flotation of cassiterite [21,23–26]. A correlation was established between the formation of the hydrolyzed species and the floatability [27,28]. Unfortunately, a typical gangue material like quartz is also activated [21,24], which makes separation more difficult, as the particles should differ in their wettability [3,9]; therefore, the activation of the chosen particle surfaces needs to be investigated in detail.

Advantageous is that the salts differ in their ability to adsorb. Indifferent electrolytes like NaCl or KCl cannot adsorb on the particle surface and lead to a compression of the electrochemical double layer (EDL) as the concentration increases, whereas multivalent ions adsorb in the Stern layer close to the particle surface, and can even generate a charge reversal [29,30]. The higher the valence of the cation, the more effective the charge reversal effect [29–32]. When investigating the adsorption of various salts on different materials, it is found that the hydrolyzed salt ions can adsorb. But for the adsorption, only a pH window can be used [33]. The adsorption of ions on the surface can be quantified using the zeta potential ζ, as the ions adsorb in the Stern layer, which has an influence on the movement of particles in an electric field, and can be determined, for example, by using electrophoretic mobility μ_e [22,29–31]. It is also recognized that some materials differ in terms of adsorption. With SiO_2, a charge reversal is only possible at pH values at which the hydrolyzed species was formed, while with SnO_2 a charge reversal was possible over a larger pH value range. It was recognized that only the hydrolyzed species of the salt-cations can adsorb on materials such as SiO_2, whereas other species, in addition to the hydrolyzed species, can adsorb on SnO_2 [12]. This can be used to create a separating feature.

With SiO_2, Weber et al. [22] have shown that $AlCl_3$ at pH 4.1 and $ZnCl_2$ at pH 8.2 can achieve a charge reversal of the particles. With $AlCl_3$, a steady increase in electrophoretic mobility μ_e was recognized until a change in its sign occurred. Further addition showed an additional increase in μ_e, indicating that adsorption in the Stern layer was not yet complete. A different behavior was shown by $ZnCl_2$, where a decrease in electrophoretic mobility μ_e was initially observed upon addition of the salt, indicating that a mobile ionic species was adsorbed in the Stern layer and that surface conductivity was also present in the Stern layer [22,34]. This was followed by an increase in the electrophoretic mobility μ_e until a change in sign occurred. $AlCl_3$ and $ZnCl_2$ required similar concentrations around 0.1 mM

for the charge reversal of SiO_2 [22]. Furthermore, charge reversal can also be achieved by surfactants [29,35] and polyelectrolytes [29] as well. In the case of surfactants, charge reversal is achieved by the formation of a bilayer, as the negative head group adsorbs to the particle surface (first layer) and faces outwards (second layer) [19].

Within the work of Weber et al. [22], they also showed that the adsorption of SDS can occur after a successful charge reversal with $AlCl_3$, which was recognized by a further change in the sign of μ_e. The mobility of the particles determined by electrophoresis is related to the zeta potential for κa >> 1, via the following Helmholtz–Smoluchowski Equation (1) [34,36]:

$$\mu_e = \frac{\varepsilon_0 \varepsilon \zeta}{\eta}. \quad (1)$$

The electrophoretic mobility μ_e is related to the zeta potential via ε, the dielectric constant of the solution, ε_0, the permittivity of vacuum, and η, the viscosity of the liquid.

Finally, in the work of Weber et al. [22], *n*-hexane was used to check whether the adsorption of SDS was sufficient to achieve a phase transfer of SiO_2. $AlCl_3$, $ZnCl_2$ and $CaCl_2$ were tested with the same amount of SDS. Phase transfer was possible in a pH range from 4 to 9.5 for $AlCl_3$, with the highest amount being transferred at pH 4, and this decreased with increasing pH. With $ZnCl_2$, a small amount of particles could always be transferred into the organic phase over the selected pH range. In comparison, all particles remained in the aqueous phase in the experiments with $CaCl_2$, as no formation of the hydrolyzed species took place in the selected pH range. This shows that charge reversal is essential for the adsorption of SDS in order to achieve the phase transfer of the particles.

The transfer of particles into the interface and into the other phase depends on several parameters. On the one hand, the wettability, size and shape of the particles have an influence and, on the other hand, the hydrophobicity or hydrophilicity of the liquids and the interfacial tension between the liquids play a decisive role. This can be summarized in the following equation of free energy of detachment $\Delta_d G$ [1,18]:

$$\Delta_d G = \pi r^2 \gamma_{OW} (1 \pm cos\theta_{OW})^2. \quad (2)$$

The γ_{OW} stands for the interfacial tension of the liquids, r for the particle radius and θ_{OW} for the wettability of the particles. The contact angles reflect the wettability of the particles. If the contact angle is less than 90°, the particles are hydrophilic; if the contact angle is greater than 90°, the particles are hydrophobic [1,18].

Figure 1 shows that it is easier for smaller particles with the same wettability to enter the interface and they require less energy to pass into the other phase. Thus, as the particle radius increases, the probability of entering the other phase decreases because either the energy is not sufficient to enter the interface, or the particle is too stable in the interface. In addition, separation into the organic phase is more favorable for hydrophobic materials than for hydrophilic ones.

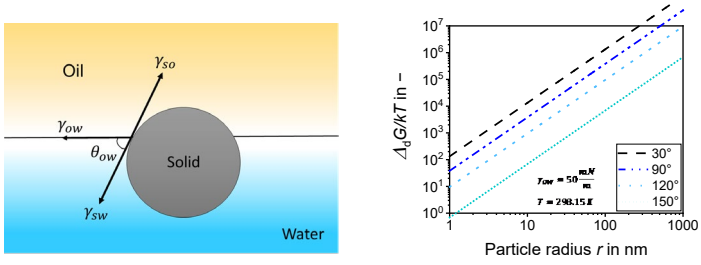


Figure 1. Particle in the interface of two immiscible liquids (**left**), and the dependence of the free energy of detachment $\Delta_d G$ as a function of the particle radius r at different contact angles θ_{OW} (**right**) according to [1,18].

In order to achieve particle separation, the selectively adsorbed metal ion can be used to form a bridge between the negatively charged particle surface and the anionic surfactant [12], creating a separation feature [37], which is characteristic of the material composition of a particle. However, as soon as a charge reversal takes place selectively on only one material, the hetero-agglomeration of the materials, which occurs between differently charged materials, has to be taken into account, which has a negative effect on the separation result [33,38]. In the case of separation by extraction, a distinction can be made between positive separation, where the target product is transferred to the concentrate/extract, and negative separation, where the target product remains as a residue in the raffinate. The liquid–liquid extraction is used to find an approach to separate the tin source (SnO_2) from the gangue material quartz (SiO_2). The influence of different salts and the surfactant SDS on the charge reversal of the particles is investigated. Furthermore, the separation of the metal oxides is analyzed under different parameters to determine the selectivity and the limitations of this approach. In order to be able to apply the approach later in industry, the process could be transferred to a continuous process, such as in a separation column [39].

2. Materials and Methods

For the experiments, two metal oxides, SiO_2 (SFP-20M and SFP-30M from Denka, Tokyo, Japan) and SnO_2 (from Carl Roth, Karlsruhe, Germany, >99.5%), were selected. NaCl (>99.0%) was obtained from Carl Roth (Germany). $ZnCl_2$ was purchased from Merck (Darmstadt, Germany, >99.0%), $AlCl_3 \cdot 6H_2O$ (99.9%), $MgCl_2$ (>99.0%) and $MnCl_2 \cdot 4H_2O$ (99.9%) were obtained from Carl Roth, Germany. The salts were utilized for the charge reversal of both metal oxides and the anionic surfactant SDS obtained from Carl Roth (Germany) with a purity of >99.0% was used for the hydrophobization of the particles. *n*-Hexane (from Carl Roth, Germany, >99.0%) was selected as the oil phase for the liquid–liquid extraction experiments. The chemicals used in the experiments were utilized without further processing. Only SnO_2 was washed with 1 mM NaCl solution and MilliQ water (PURELAB® Ultra, ELGA LabWater, Celle, Germany). All solutions were prepared with MilliQ water. For the experiments where the Zetasizer Nano ZS was used, the solutions were made with MilliQ water (MilliQ RefA+, Merck, Germany).

2.1. Particle Characterization

SiO_2 SFP-20M and SnO_2 were characterized by different methods. The following Figure 2 shows TEM images of the metal oxides. It becomes obvious that the particles shown fulfill the requirements of being smaller than 1 µm. However, it is also apparent that the particles differ in shape.

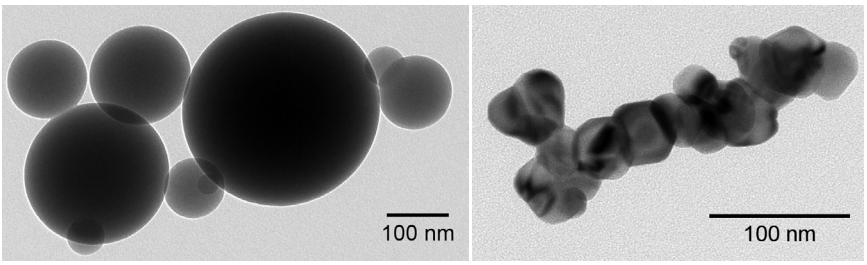


Figure 2. TEM pictures of SiO_2 SFP-20M (**left**) and SnO_2 (**right**).

2.1.1. Particle Size Distribution

The particle size was determined in an aqueous solution using dynamic light scattering (DLS) using the Nanophox (Sympatec, Clausthal-Zellerfeld, Germany). TNPP with a mass

concentration of 1 g/L was used to stabilize the particles. The particles were added to the TNPP solution and dispersed with the sonotrode (SONOPULS with type UW 2200, BANDELIN electronic GmbH & Co. KG, Berlin, Germany) for 2 min at 50%. A sample was then placed in a measuring cuvette and measured for 120 s. The particles were measured three times. The particle size distributions for the different metal oxides and the 1:1 mixture of SiO_2, SFP-20M and SnO_2 are summarized in Figure 3 below.

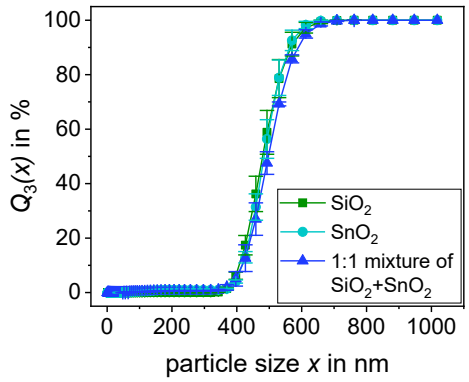


Figure 3. Particle size distribution $Q_3(x)$ for SiO_2 SFP-20M, SnO_2 and the 1:1 mixture of SiO_2 SFP-20M and SnO_2. The data points show the average of three values and the bars represent the calculated standard deviation.

Figure 3 shows that the two metal oxides used, SiO_2 SFP-20M and SnO_2, do not differ significantly from each other. As a result, the particle size distribution of the 1:1 mixture of SiO_2 and SnO_2 does not differ from that of the pure materials. This can also be seen in the following Table 1 using the x_{10}, x_{50} and x_{90} values.

Table 1. Summary of x_{10}, x_{50} and x_{90} values for SiO_2 SFP-20M, SnO_2 and the 1:1 mixture of SiO_2 SFP-20M + SnO_2.

	SiO_2	**SnO_2**	**1:1 Mixture of SiO_2 + SnO_2**
x_{10} in nm	407.8 ± 5.2	417.6 ± 6.2	416.9 ± 14.4
x_{50} in nm	480.4 ± 11.0	485.1 ± 9.2	496.4 ± 5.9
x_{90} in nm	565.4 ± 20.5	561.8 ± 15.3	589.7 ± 7.0

As can be seen from Table 1, the 1:1 mixture of SnO_2 and SiO_2 is slightly coarser, which can be explained by the fact that the particles agglomerate faster than the pure materials due to the different charges. According to Weber et al. [22], the SiO_2 SFP-30M used has a particle size between 0.1 and 2 µm with a mean diameter of 0.6 µm and is therefore coarser than the SiO_2 SFP 20M, which was preferred.

2.1.2. Determination of the Specific Surface Area According to BET S_{BET}

The specific surface area of the metal oxides was determined using Gemini VII (Micromeritics GmbH, Unterschleißheim, Germany) with the Gemini VII Version 5.00 software. Before starting the measurement, the samples were heated at 200 °C under vacuum. After heating, the mass of the sample was measured. The specific surface areas of three samples were determined in order to calculate an average and a standard deviation. For the mixture, equal amounts of SiO_2 SFP-20M and SnO_2 were weighed, mixed and then divided using a sample divider. The values obtained are summarized in Table 2 below.

Table 2. Summary of the specific surface areas according to BET for the values for SiO_2 SFP-20M, SnO_2 and the 1:1 mixture of SiO_2 SFP-20M + SnO_2.

Material	S_{BET} in m^2/g
SiO_2	10.05 ± 0.01
SnO_2	6.70 ± 0.06
1:1 mixture of SiO_2 + SnO_2	8.27 ± 0.08

2.1.3. Calculation of the Concentration Needed to Cover the Particles with the Different Ions and SDS

The size of the ions is important in order to calculate the quantity of ions required to completely cover the particles. Effective ion radii [40–43], ion radii in the crystal [44] and atomic radii [42] of the metals can be found in the literature. The method used to determine the ion radii, which was used for further calculations, is X-ray diffraction, in which an electron density distribution is obtained [43]. The minimum of the electron density distributions between the anions and cations under investigation is used as the limit for the calculation, for which the ionic radius of the anion or cation must also be known [42,43]. For the calculation of the ion radii, F^- = 1.19 Å was used as a reference, so that the ion radii are related to this [43,45]. Please note that the radii used were determined with F^- as a reference.

The ionic radius depends on the element, the charge and the coordination number (CN). The parameters important for the calculation, such CN, ion radius and the molar mass are summarized in the following Table 3 for the ions used. Since the metal ions in the water are differently coordinated, the corresponding ionic radii of the respective coordination numbers were used for the calculations.

Table 3. Summary of the important parameters, coordination number (CN), ion radius r_{Ion} in Å and the molar mass M in g/mol.

Ions	CN	r_{Ion} in Å	M in g/mol
Al^{3+}	6 [42]	~0.54 [42,44,45]	27.0
Mg^{2+}	6 [42]	0.72 [41,42,44]	24.3
Zn^{2+}	6 [45]	0.74 [44,45]	65.4
OH^-	2 [45]	1.32 [44,45]	17.0

The specific surface areas assumed for the metal ions were calculated using the ion radii in Table 3. The specific surface area according to BET $S_{BET,}$ which corresponds to $S_{m,}$ was used as the basis for the calculated particle coverage. The equations for the calculation for the ions are shown below. First, the number of molecules for 1 g of metal oxide was calculated. This requires the area of the ions A_{Ion}.

$$Molecules\ per\ g\ metal\ oxide = \frac{S_{BET}}{A_{Ion}} \quad (3)$$

The molecules per g metal oxide are given in g^{-1}.

$$Amount\ of\ Ions = \frac{M_{Ion}}{N_A} \cdot Molecules\ per\ g\ metal\ oxide, \quad (4)$$

with N_A = 6.022·10^{23} mol^{-1} as the Avogadro constant.

Table 4 summarizes the calculated amounts in mg required to cover 1 g of particles. The standard deviations result from the fact that the BET specific surface area was determined

three times. The specific amounts were then calculated for each value to obtain a mean and a standard deviation.

Table 4. Calculated quantities required for complete covering of 1 g particles.

Ions	Calculated Quantities Required for the Complete Covering of 1 g Particles for:		
	Coverage of SiO_2 in mg	**Coverage of SnO_2 in mg**	**Coverage of 1:1 Mixture of SiO_2 + SnO_2 in mg**
Al^{3+}	49.2 ± 0.1	32.8 ± 0.3	40.5 ± 0.4
Mg^{2+}	24.9 ± 0.0	16.6 ± 0.2	20.5 ± 0.2
Zn^{2+}	63.5 ± 0.1	42.3 ± 0.4	52.2 ± 0.5
SDS	9.6 ± 0.0	6.4 ± 0.1	7.9 ± 0.1

By calculating the amount required to cover 1 g of particles entirely, it becomes clear that the BET of the materials has a major influence, and a higher quantity is always required for SiO_2 than for SnO_2. The mixture provides the approximate mean value of the required quantities of SiO_2 and SnO_2. Furthermore, the molar mass and the ionic radius have a major influence. Although Zn^{2+} and Mg^{2+} have a similar ionic radius but the molar mass of Zn^{2+} with 65.4 g/mol differs strongly from Mg^{2+} with 24.3 g/mol. This explains the large deviation in the required amounts, which is especially true for the molar mass of the SDS used rather than the actual adsorbing sulfate ion.

2.2. Formation of the Hydrolyzed Species

With the aid of the software ChemEQL V3.1 [46], different salts were investigated to determine the occurrence of the hydrolyzed species. For each salt, the formation of the hydrolyzed species differs with regard to pH value and concentration. A starting concentration of 0.5 mM was used for each salt. The formation of the main and positively charged hydrolyzed species for all investigated salts are shown in Figure 4.

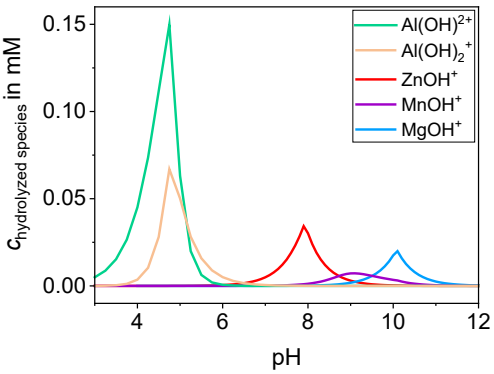


Figure 4. The concentration of the hydrolyzed species of different metal ions, the hydrolyzed species Al^{3+} (green and yellow), the hydrolyzed species of Zn^{2+} (red), hydrolyzed species of Mn^{2+} (violet) and the hydrolyzed species of Mg^{2+} (blue), for a 0.5 mM salt solution calculated with ChemEQL [46].

The maximum concentration of the hydrolyzed species for Al^{3+} occurs between pH 4.1 and 4.5, for Zn^{2+} around pH 8, for Mn^{2+} the maximum is at pH 9 and for Mg^{2+} the maximum occurs at pH 10. This means that different salts are available at different pH values for a possible charge reversal of the target particle systems.

2.3. Determination of the Zeta Potential ζ via Electroacoustic Measurements

For the determination of the zeta-potential ζ, the AcoustoSizer II (Colloidal Dynamics LLC, Ponte Vedra Beach, FL, USA) is used. The metal oxide was added to a 150 mL

1 mM NaCl solution and dispersed with a sonotrode (SONOPULS with type UW 2200, BANDELIN electronic GmbH & Co. KG, Berlin, Germany). To ensure that the adsorption of the hydrolyzed metal cations can be investigated, the indifferent electrolyte NaCl is used as a background electrolyte. For this reason, the chlorides of the metal cations were used as salts. The suspension was then transferred to a storage vessel. The stirrer (MINISTAR 20 digital, IKA, Staufen, Germany) was used to prevent the sedimentation of the sample and mixing. The pump (MasterFlex™ L/S modular precision pumping systems, Cole-Parmer™, Vernon Hills, IL, USA) was used to transfer the sample to the ESA sensor.

Different amounts of salt solution were added to determine charge reversal. The acid HCl and the base NaOH were chosen to correspond to the NaCl. The acid and the base were used at a concentration of 0.1 M or 1 M to adjust the pH value. Three measurements were made for each salt concentration, and the average value was calculated. The zeta potential ζ according to Smoluchowski was used for the evaluation.

2.4. Determination of the Zeta Potential ζ via Electrophoresis Measurements

A 1 mmol/L (mM) NaCl solution was used as the background electrolyte. First, the particles were dispersed in the electrolyte for 2 min using a sonotrode (SONOPULS with type UW 2200, BANDELIN electronic GmbH & Co. KG, Berlin, Germany). The suspension was then transferred to a double-walled beaker and tempered to 25 °C while stirring with the ECO RE 415 thermostat (Lauda, Germany). The samples were then measured in folded capillary cells (DTS1070) at 25 °C in the Zetasizer Nano ZS (Malvern, Germany). The measurement was performed with 25–100 sub-runs and a drive voltage of 40 V. Each data point consists of 3 measurements, and an average and a standard deviation could be determined from these. The zeta potential according to Helmholtz–Smoluchowski was used for the evaluation. The pH values for the pH titrations were adjusted with 1 M or 0.1 M of NaOH or HCl and carried out in a range from pH 4 to pH 10. For the pH titrations with the salts, an initial concentration of salt was set and then the pH values were adjusted also with 1 M or 0.1 M of NaOH or HCl and carried out in a range from pH 4 to pH 10.

Figure 5 shows the pH titration of SiO_2 SFP-20M, SFP-30M and SnO_2. It shows that the isoelectric point of SnO_2 is close to pH 4. The isoelectric point of SiO_2 could not be determined as it was not within the measuring range. The isoelectric point of SiO_2 is described in the literature at below pH 3 [47].

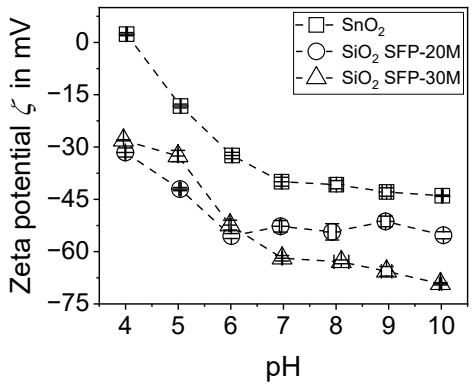


Figure 5. pH titration of SiO_2 SFP-20M, SiO_2 SFP-30M and SnO_2 in 1 mM NaCl solution to determine the isoelectric point. The data points show the average of three values and the bars represent the calculated standard deviation.

2.5. Liquid–Liquid Extraction and Separation of the Particles

The same experimental setup was used for both the liquid–liquid extraction and the separation of the particles using the liquid–liquid extraction. The liquid–liquid extraction for the pure materials is shown in Figure 6 and the separation is shown in Figure 7.

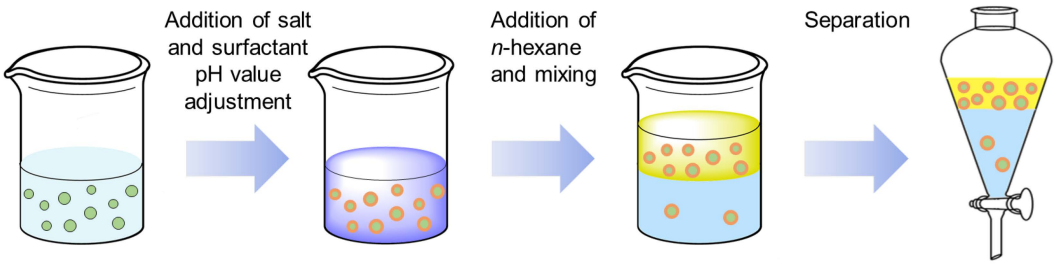


Figure 6. Schematic representation of liquid–liquid extraction using SiO_2 as an example.

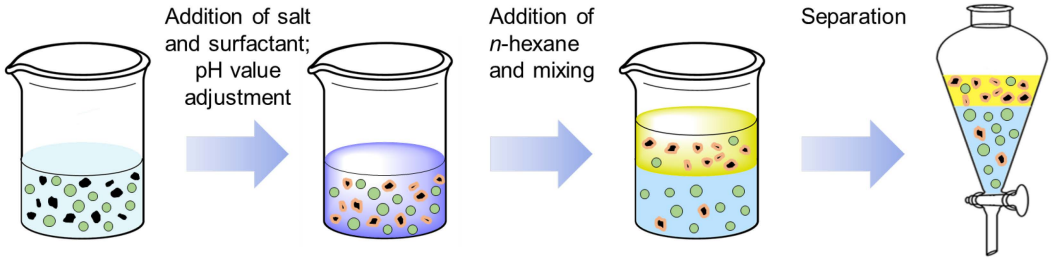


Figure 7. Schematic representation of separation of SiO_2 (green) and SnO_2 (black) using liquid–liquid extraction.

For this purpose, the particles were weighed according to the desired solids concentration of the pure materials or material mixtures, which range from 5 g/L to 20 g/L. After the addition of 150 mL MilliQ water as polar liquid, the particles were dispersed using an Ultra-Turrax from IKA (with dispersing unit S 25 N–25 F) at 6500 rpm for 5 min. While stirring the suspension, the specified amount of $ZnCl_2$ or $MgCl_2$ was added first, followed by SDS. The specific adsorption of the ions and thus the hydrophobization is represented by the orange contour. After the addition of all components, the pH value was adjusted with 0.1 M or 1 M HCl or NaOH. In the next step, 25 mL of non-polar liquid *n*-hexane for extraction was added and the phases were mixed with the Ultra-Turrax at 6500 rpm for 5 min. The difference in density between the aqueous and oil phases allows for separation in a separation funnel. The hydrophobic particles were separated with the *n*-hexane phase, while the hydrophilic particles remained in the aqueous phase. Due to the immiscibility and density differences between *n*-hexane and water, the phases and the particles in them can be separated at the interface between the phases. The mass recovery R_m was determined after drying and weighing the samples. The mass of particles that have passed into the organic phase is defined as m_c (Index c for concentrate) and the mass of particles that remain in the aqueous phase is defined as m_r (Index r for reject).

$$R_m = \frac{m_c}{m_c + m_r} \cdot 100\%. \quad (5)$$

Based on previous experiments [12], the separation tests are carried out at pH 6 and pH 8. To determine the efficiency of the separation, it is important to know the composition of the particles that passed into the organic phase and the particles that remained in the aqueous phase. The grades of the individual oil phase ($c_{1,c}$; $c_{2,c}$) were determined using XRF. The composition of the particles remaining in the aqueous phase was calculated using the following equations, as the masses obtained were too low for XRF analysis. The mass

of the metal oxide (MeO_2) $m_{MeO2,Oil/H2O}$ in this case for SiO_2 or SnO_2, in the oil or aqueous phase, is calculated with the grade of the SiO_2 or SnO_2 c_{MeO2}. $m_{ges,Oil}$ describes the mass of particles that have passed into the organic phase and $m_{ges,H2O}$ describes the mass of particles remaining in the aqueous phase. Since artificial mixtures were used, the total mass fraction of the metal oxides $m_{MeO2,ges}$ is known. Therefore, the remaining mass fraction in the aqueous phase $m_{MeO2,H2O}$ can be calculated with the determined mass fraction in the oil phase $m_{MeO2,Oil}$.

$$m_{MeO_2,Oil/H_2O} = c_{MeO_2} \cdot m_{ges,Oil/H_2O}, \quad (6)$$

$$m_{MeO_2,H_2O} = m_{MeO_2,ges} - m_{MeO_2,Oil}. \quad (7)$$

The main parameters of the evaluation are summarized in Figure 8. The grades $c_{1,s}$ and $c_{2,s}$ are the concentrations of SiO_2, which obtained an index of 2 (Figure 7: green spherical particles) and SnO_2 as the valuable material (Figure 7: black irregularly shaped particles), obtained an index of 1, in the supply (s). Because the mixture used is a 1:1 mixture of SiO_2 and SnO_2, $c_{1,s}$ and $c_{2,s}$ are 50% (m/m). $R_{m,c}$ is equal to the received mass recovery of the organic phase (c—concentrate) and $R_{m,r}$ is equal to the received mass recovery in the aqueous phase (r—reject) [48]. As the quantities of salt and surfactants added are negligible, the quantities are not taken into account when calculating the yield.

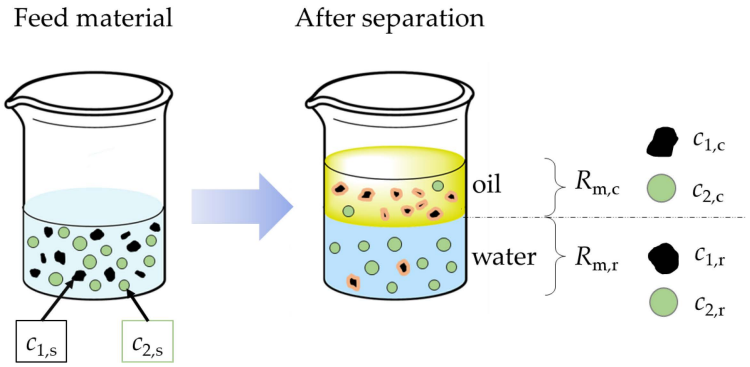


Figure 8. Parameters for the evaluation of the separation, whereby the green spherical particles represent SiO_2 and black irregular shaped particles SnO_2.

The following Equation (8) to Equation (9) were used for the evaluation to calculate the specific mass recoveries $R_{1,c}$; $R_{1,r}$; $R_{2,c}$ and $R_{2,r}$ for SnO_2 (Index 1) and SiO_2 (Index 2) for the reject (Index r) and the concentrate (Index c). Therefore, the concentrations (c; grades) of the materials are used in the following:

$$R_{1,c/r} = R_{m,c/r} \frac{c_{1,c/r}}{c_{1,s}}, \quad (8)$$

$$R_{2,c/r} = R_{m,c/r} \frac{100 - c_{1,c/r}}{100 - c_{1,s}}. \quad (9)$$

2.6. Determination of the Material Content via XRF Measurements

For the XRF analysis, the dried samples were crushed with a porcelain mortar. The samples were then filled into sample tubes (diameter of 32 mm) sealed with a polypropylene film from analyticon instruments gmbh (Rosbach v. d. Höhe, Germany). The samples were analyzed using the handheld XRF device Niton XL5 plus (analyticon instruments gmbh, Germany). The samples were shaken after each measurement and each sample was measured five times and averaged to obtain a representative value. Since the Niton connect XRF software version 2.5.2.1589 only gives the elemental composition, the oxides were calculated using the correction factor f for Sn → SnO_2 1.2695 and f for Si → SiO_2 2.1393 [49].

In addition, the values were corrected using the linear equation of the calibration curve for SiO_2 (y = 1.07x + 0.05) and SnO_2 (y = 0.58x + 0.01) with a linear fit of R^2 of 0.9969 for SnO_2 and 0.9982 for SiO_2. The y value represents the XRF measured metal oxide content in % (m/m) and the x value represents the theoretical content in % (m/m). The calculated x value is then used for evaluation. All values are normalized to 100% (m/m) since the compositions of the artificially prepared mixtures are known.

3. Results

3.1. Investigations for the Charge Reversal of Particles

As shown in Figure 5, the particles are negatively charged over a wide pH range. The adsorption of ions of the selected salts changes the charge around the particle. This can be observed by the change in zeta potential as a function of ion concentration, which correlates with the occupancy of the particles. The adsorption of the salts should result in a positive sign of the zeta potential ζ. Various salts such as $AlCl_3$, $MgCl_2$, $MnCl_2$ and $ZnCl_2$ were studied for the charge reversal experiments, because they form hydrolyzed species at different pH values. For the charge reversal, pH 4 was selected for Al^{3+}, pH 8.2 and later pH 8 for Zn^{2+}, pH 9 for Mn^{2+} and pH 10 for Mg^{2+}. This means that different salts are available at different pH values for a possible charge reversal of the target particle systems. Due to the IEP of SnO_2 close to pH 4, only $MgCl_2$, $MnCl_2$ and $ZnCl_2$ are suitable.

The zeta potential ζ is used to study the adsorption behavior of different salts. For the separation, only one of the materials achieves a charge reversal, while the other remains negatively charged. This can then be followed by the selective adsorption of the surfactant, in this case SDS. A second reverses of the sign of the zeta potential ζ occurs, so that it is negative. Because of this, selective hydrophobization can be achieved. This is important for creating a selective separation.

3.1.1. Investigations with the Aid of Electroacoustics

As described in Section 2.1, there are several salts that could be used for the charge reversal of the materials. First, the adsorption of $AlCl_3$ on SiO_2 was investigated at different mass concentrations of SiO_2. A pH 4 according to Weber et al. [22] was selected, as this is where the hydrolyzed species can occur (Figure 4).

Figure 9 shows the dependence of the zeta potential on the addition of $AlCl_3$ to a SiO_2 SFP 30M suspension at pH 4. The zeta potential ζ initially increases rapidly when increasing of the concentration of the Al-ions. This is followed by a shallower rise, which indicates that the ions already adsorbed in the Stern layer slow down the adsorption, as the same charges interfere with each other. A charge reversal is possible for all three selected mass concentrations of SFP 30M, although the amounts of $AlCl_3$ required are different, due to the different volume-related specific surface areas $S_{v.}$ The amount of 0.11 mM was required for 1% (m/m), 0.18 mM for 3% (m/m), and 0.30 mM for 5% (m/m), however, there is no proportionality between S_v and c_{AlCl3}.

As described in Section 2.1.2, the amount of SiO_2 SPF 30M required to fully occupy the mass concentration of the particles can be calculated. This S_{BET} for the material is 2.4 m^2/g. Due to the larger ionic radii of the hydrolyzed species, a lower concentration of these ions is required to occupy the particles.

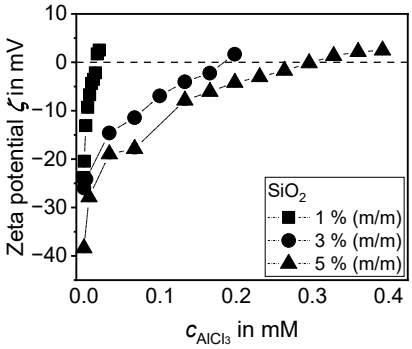


Figure 9. Zeta potential ζ of SiO_2 SFP 30M as a function of the $AlCl_3$ concentration for different mass concentrations of SiO_2 at pH 4 measured with electroacoustic measurements. The data points show the average of three values and the bars represent the calculated standard deviation.

Table 5 shows the importance of knowing the ions in the solution. Unfortunately, the literature does not indicate if Al^{3+} can also be adsorbed or if only the two hydrolyzed species adsorb. However, the amount of Al^{3+} that is theoretically required for complete occupancy and is thus close to charge reversal is significantly higher than the concentration experimentally required for actual charge reversal. If the quantities of the hydrolyzed species are added together, 1% (m/m) is the approximate quantity required for charge reversal. The higher the particle concentration, the greater the difference between the theoretical and actual concentration required.

Table 5. Amounts of Al^{3+} and its hydrolyzed species required for the occupancy of different mass concentrations of SiO_2 SFP 30M.

Species	r_{Ion} in Å	Requirement for the Individual Ions in mM for:		
		1% (m/m)	3% (m/m)	5% (m/m)
Al^{3+}	0.54	0.49	1.46	2.43
$Al(OH)^{2+}$	1.86	0.07	0.20	0.33
$Al(OH)_2{}^{+}$	3.18	0.03	0.10	0.16
Experiment $AlCl_3$		0.11	0.18	0.30

This indicates that the initial dispersion of the particles may not be sufficient and, in addition, that they are likely to agglomerate over the measurement time due to the decreasing potentials that correlate with the lower repulsion. The agglomeration increases with the increasing particle concentration.

Unfortunately, $AlCl_3$ is not suitable for a charge reversal of SnO_2 as the IEP (Figure 5), which is near pH 4, is too close to the pH of the hydrolyzed Al-species. Consequently, the SnO_2 has no negative surface charges at this pH value and no adsorption of the hydrolyzed Al species would be possible. For this reason, other salts are investigated, as the salts need to form a hydrolyzed species above the IEP of the materials. Therefore, $ZnCl_2$, $MnCl_2$ and $MgCl_2$ are considered.

Figure 10 shows the different charge reversal curves for SnO_2 (left, empty symbols) and SiO_2 (right, full symbols) for different salts for the respective pH values (Figure 4), which shows the charge reversal for SiO_2 and SnO_2 that only works for two of the three salts. The ChemEQL calculations also showed that the highest amount of hydrolyzed ions for $ZnCl_2$ is produced at pH 8.2, and the formation of $ZnOH_2$ also starts at this pH value, resulting in a precipitate.

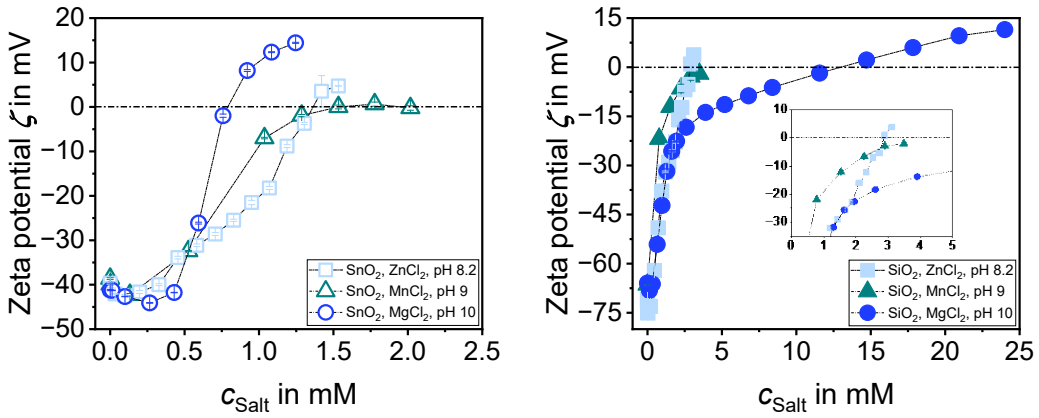


Figure 10. Zeta potential ζ of SnO_2 (left) and SiO_2 SFP 20M (right) as a function of the salt concentration for different pH-values with 5% (m/m). The data points show the average of three values and the bars represent the calculated standard deviation.

The charge reversal of SiO_2 is possible with $ZnCl_2$ at pH 8.2 at 2.86 mM and with $MgCl_2$ at pH 10 at 12.98 mM. Furthermore, for SnO_2 at pH 8.2, a charge reversal can be achieved with 1.36 mM of $ZnCl_2$ and at pH 10 with 0.79 mM of $MgCl_2$. The curves are similar to the curves shown in Figure 9. It can be seen from this that SnO_2 always requires lower quantities of salt than SiO_2, which can be explained by the different IEPs shown in Figure 5. SiO_2 has an IEP of pH < 3, which is known from the literature, while the IEP of SnO_2 is close to pH 4. This results in a difference in the amount of salt required for the investigated pH values.

As described by Weber et al. [22] for SiO_2 SFP 30M, all curves at SnO_2 first pass through a minimum before the zeta potential increases. According to Delgado et al., this indicates the adsorption of a mobile species in the Stern layer and that surface conductivity is also present in the Stern layer [22,34]. Subsequently, the zeta potential increased rapidly with increasing ion concentration. This was followed by a shallower increase, indicating the charge already adsorbed in the Stern layer, which prevents adsorption because like charges interfere with each other. The presence of a mobile species in the Stern layer or a surface conductivity in the Stern layer could not be confirmed for SiO_2 SFP 20M. A rapid increase in the zeta potential was observed for all salts, which later flattened. This indicates that ions are already adsorbed in the Stern layer and slow down the adsorption, as the same charges interfere with each other. A completely different behavior is shown in $MnCl_2$. Initially, the hydrolyzed species adsorbs in the Stern layer, causing the zeta potential to rise. However, no charge reversal is achieved, because the $MnCl_2$ oxidizes during the measurements, which could be seen from the brownish discoloration of the white suspension. The oxidized form reduces the amount of free $MnCl_2$ and, therefore, the source of the hydrolyzed species and concentration also decreases. For this reason, no charge reversal is achieved, and the zeta potential starts to decrease after a while and thus shows a clear time dependency. Apparently, this phenomenon only occurs with oxides, because a charge reversal with $MnCl_2$ at pH 9 was observed for CdS [39]. The oxidation of Mn^{2+} could not be prevented due to the use of metal oxides and non-degassed liquids [50]. Furthermore, it was not possible to work inertly due to the nature of the devices, i.e., oxygen was always present during the measurement. As the presence of oxidized Mn^{2+} on the particle surface hinders particle separation, this separation approach was rejected.

Table 6 summarizes the calculated quantity required to completely occupy the particles with ions as well as the concentrations required for the charge reversal. It is clear that a significantly lower salt concentration must be used than that theoretically calculated with the ionic radius of the salts, which is shown in Table 6. This can be explained by the

agglomeration of the particles during the addition of the salts, as the value of the potential decreases, and thus the repulsion of the particles decreases. And theoretically, one would expect the theoretical concentration to be lower than the actual concentration required, since some ions are still in solution, while others are adsorbed on the particle surface.

Table 6. Amounts of Zn^{2+} and Mg^{2+} with their hydrolyzed species required for the occupancy of 5% (m/m) SiO_2 SFP 20M and SnO_2.

Species	r_{Ion} **in Å**	**Required Concentration for the Individual Ions in mM for:**	
		SnO_2 5% (m/m)	**SiO_2 5% (m/m)**
Zn^{2+}	0.74	16.34	24.53
$Zn(OH)^+$	2.06	2.66	3.99
Experiment $ZnCl_2$		1.36	2.86
Mg^{2+}	0.72	9.18	13.7
$Mg(OH)^+$	2.04	1.94	2.92
Experiment $MgCl_2$		0.79	12.98

For manganese, this was not calculated because the charge reversal did not work and in addition, there are six oxidation states with different coordination numbers, so there are too many variables for clear determination.

Since the influence of the precipitation of $ZnCl_2$ is not known, the pH value of 8 was used for the electrophoretic measurements, which were published in Heilmann et al. [12].

3.1.2. Investigations with the Aid of Electrophoresis

Another method of determining the zeta potential ζ is electrophoresis. The difference between electrophoresis and electroacoustics is that significantly smaller quantities of particles can be used within the electrophoresis method. The influence of low particle concentrations should be investigated. These results have already been published in Weber et al. [22] and Heilmann et al. [12]. It was found that SnO_2 and SiO_2 differ significantly in terms of their adsorption properties. It was assumed that the charge reversal of the materials is only possible when the hydrolyzed species of the salts are formed, which occurs at pH 7–9 for Zn^{2+} and pH 9–11 for Mg^{2+}, pH titrations for SnO_2 and SiO_2 with $ZnCl_2$ (Figure 11, left) and with $MgCl_2$ (Figure 11, right), which were performed and are shown below. Different initial concentrations of the salts were selected for this in order to achieve a charge reversal.

There is a clear difference between SiO_2 and SnO_2, particularly at pH values of 4 to 7. The reason for this is that if there are no hydrolyzed metal cations, there is no charge reversal for SiO_2, whereas a charge reversal occurs for SnO_2 in this pH range, because the SnO_2 surface can adsorb non-hydrolyzed metal ions. This pH titration revealed that specific adsorption only occurs for SiO_2 at pH 8 and pH 9, and this is mainly due to the better adsorption capacity of the hydrolyzed $ZnOH^+$ species. For SnO_2, a charge reversal also occurs at pH 8 and pH 9. The adsorption of non-hydrolyzed species explains why SnO_2 at pH 8 requires significantly less $ZnCl_2$ for a charge reversal than SiO_2, as SnO_2 adsorbs both hydrolyzed metal ions and non-hydrolyzed metal ions. At pH 10, Zn^{2+} precipitates as $Zn(OH)_2$ and the value of the zeta potential decreases, which applies to both metal oxides.

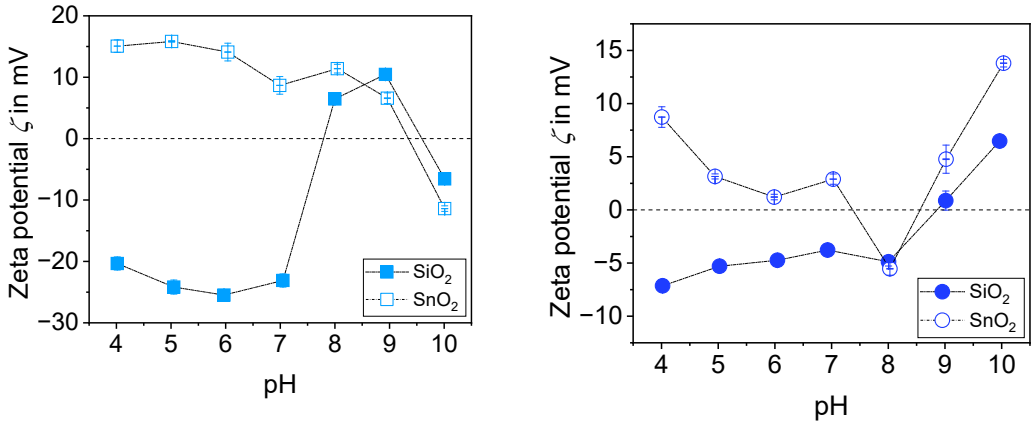


Figure 11. pH titration with $ZnCl_2$ for SiO_2 with c_{ZnCl_2} = 0.79 mM and for SnO_2 with c_{ZnCl_2} = 0.30 mM (left) with $MgCl_2$ for SiO_2 with c_{MgCl_2} = 12.3 mmol/L and for SnO_2 with c_{MgCl_2} = 0.40 mM (right). Curves with μ_e are already published in Heilmann et al. [12]. The data points show the average of three values and the bars represent the calculated standard deviation.

This was also observed approximately for $MgCl_2$ (Figure 11, right). A charge reversal could be obtained for SiO_2 at a specific adsorption of the hydrolyzed $MgOH^+$ species at pH 9 and pH 10, whereas for SnO_2 a charge reversal was observed over a wider pH range due to the possibility to adsorb non-hydrolyzed species. The zeta potential of SnO_2 only becomes negative at pH 8 and the concentration of the adsorbable species at this pH is insufficient to achieve charge reversal. The fact that SnO_2 is well suited for the adsorption of metal cations has already been described in the literature [51]. In summary, it can be concluded that the surface of SiO_2 is not suitable for the adsorption of non-hydrolyzed species compared to SnO_2.

3.2. Liquid–Liquid Extraction of SiO_2 and SnO_2

In the adsorption experiments with electrophoresis, a further charge reversal is observed, originating from SDS on the particle surface, which already had a first charge reversal with the salt [12], allowing the hydrophobization of the particles and the quantification in the liquid–liquid extraction of the pure materials. It was assumed that similar curves would be obtained as with the pH titration in the salts, because only a recharged particle surface should allow the adsorption of the dodecyl sulfate ion (DS^-).

Figure 12 shows the mass recoveries R_m for the liquid–liquid extraction of SiO_2 and SnO_2 at different pH values. The results for $ZnCl_2$ are shown on the left and for $MgCl_2$ on the right. As expected, the highest yields are at pH 8 with 88.3 ± 3.4% for SiO_2 and 99.0 ± 0.1% for SnO_2. As already observed in the pH titration in the $ZnCl_2$ solution, the adsorption of Zn^{2+} ions on the particle surface of SnO_2 is also possible at pH 6. A high yield is obtained at pH 4, as the DS^- ion can adsorb on the positively charged surface due to the IEP of SnO_2 at approximately pH 4. In comparison, SiO_2 shows a selective behavior, so that only low yields are obtained at the other pH values. The influence of the correct $ZnCl_2$ dosage is shown by the data point at pH 8 for the selected $ZnCl_2$ concentration of 0.1 mM, as only a concentration of 7.2 ± 1.0% was achieved for SiO_2.

In the experiments with $MgCl_2$ as a salt, the selectivity decreases, which is particularly evident with SiO_2. This suggests that the adsorption of the hydrolyzed species is also possible at higher pH values. For SnO_2, the liquid–liquid extraction experiments show a high yield over the entire pH range. In contrast to SnO_2, SiO_2 needs a significantly higher $MgCl_2$ concentration. Because even if the $MgCl_2$ concentration for SiO_2 is used at pH 10, which was used for SnO_2 (c_{MgCl2} = 0.25 mM), the quantity is not sufficient to achieve a charge reversal of the SiO_2 particles and thus enable adsorption of SDS, because only a

yield of 10.8 ± 2.9% is achieved. It was also noted that the SiO_2 samples, which were mixed with a higher concentration of $MgCl_2$ absorbed water after drying, indicate the formation of $MgCl_2 \cdot 6H_2O$.

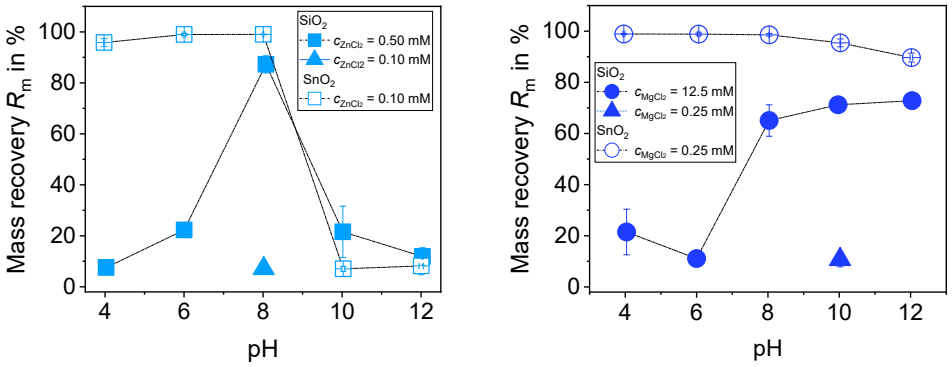


Figure 12. Mass recovery R_m of liquid–liquid extraction of SiO_2 and SnO_2 with the aid of $ZnCl_2$ and SDS (for SiO_2 c_{ZnCl2} = 0.5 mM & c_{ZnCl2} = 0.1 mM and for SnO_2 c_{ZnCl2} = 0.1 mM, each with c_{SDS} = 0.25 mM) (left) and with the aid of $MgCl_2$ and SDS (for SiO_2 c_{MgCl2} = 12.5 mM & c_{MgCl2} = 0.25 mM and for SnO_2 c_{MgCl2} = 0.25 M, each with c_{SDS} = 0.25 mM) (right). As this was already published in Heilmann et al. [12], only the values for SiO_2 with the lower salt concentration were added. The data points show the average of three values and the bars represent the calculated standard deviation.

Different salt concentrations were used in the experiments in order to achieve a transfer of the particles and to demonstrate the influence of the salt concentration, the lower concentration for SiO_2 was used at pH 8 for $ZnCl_2$ and at pH 10 for $MgCl_2$. As with the pH titration with the salts, the experiments also showed that the materials differ greatly in their adsorption behavior. This can be attributed to the ability of SnO_2 to adsorb non-hydrolyzed species in addition to the hydrolyzed species. The fact that the materials used differ in their adsorption properties has the advantage that the separation can also be controlled via the pH value as well as via the amount of salt. pH 6 was chosen, as the differences in the yield and in the zeta potential were maximized at this pH value. In addition, pH 8 was also chosen to find out whether the separation can be controlled via the $ZnCl_2$ concentration.

3.3. Separation of SiO_2 and SnO_2

The differences in the parameters were therefore used to generate a specific separation characteristic to separate the two materials. Two parameters are used to evaluate the separation, the purity of the phases (grade) and the mass recovery of the particles. For this reason, grade recovery curves are presented [48]. The specific recoveries were calculated with Equations (8) and (9). The grades were determined with the XRF for the oil phase and for the aqueous phase calculated with Equations (6) and (7). During separation, SnO_2 should pass into the organic phase while SiO_2 remains in the aqueous phase, as summarized in Figure 7. For this reason, the grades and recoveries for the organic phase are shown for SnO_2 (left) and the grades and recoveries for SiO_2 are shown for the aqueous phase (right).

In Table 7, the concentration for the material required to completely cover the particles is summarized. Two different surfactant concentrations are used for the separation, whereby 0.1 mM is just sufficient to occupy the particles and the other, c_{SDS} = 0.25 mM, has an excess. Two SDS concentrations were chosen because how the particles enter the organic phase, whether the hydrophobicity is sufficient or whether the SDS still has a supporting effect, are unknown. In addition, it is not known whether the hydrophobic particles are sufficient to stabilize the emulsion droplets or whether SDS also has a supporting effect.

Table 7. Amounts of Zn^{2+} and Mg^{2+} with their hydrolyzed species required and SDS for the occupancy of 0.75 g SiO_2 SFP 20M, SnO_2 and 1:1 mixture of SiO_2 + SnO_2 related to the molar mass of the chlorides.

Species	Required Concentration for the Individual Ions in mM for:		
	SnO_2	SiO_2	1:1 Mixture of SiO_2 + SnO_2
Zn^{2+}	1.55	2.33	1.92
$Zn(OH)^+$	0.25	0.38	0.31
Mg^{2+}	0.87	1.31	1.08
$Mg(OH)^+$	0.18	0.28	0.23
SDS	0.11	0.17	0.14

To ensure that the mass balance is correct, the values for the composition of the aqueous phase were calculated using Equations (6)–(9).

3.3.1. Separation of a 1:1 Mixture of SiO_2 and SnO_2 with $ZnCl_2$ (0.5% (m/m))

Several parameters were analyzed for the separation of SiO_2 and SnO_2, varying the amount of salt and surfactant at pH 6 and pH 8. The results for pH 6 (Figure 13) and pH 8 (Figure 14) are shown below. Previous experiments (Figure 12) have shown that the largest deviation in the mass recovery R_m of the materials occurs at pH 6, as no charge reversal of SiO_2 takes place at pH 6. pH 8 was chosen because a charge reversal of both materials takes place at this pH value, and it can therefore be checked whether the separation can be controlled via the concentration of $ZnCl_2$ and SDS. The aim of the liquid–liquid extraction is that SnO_2 should pass into the organic phase, while SiO_2 should remain in the aqueous phase.

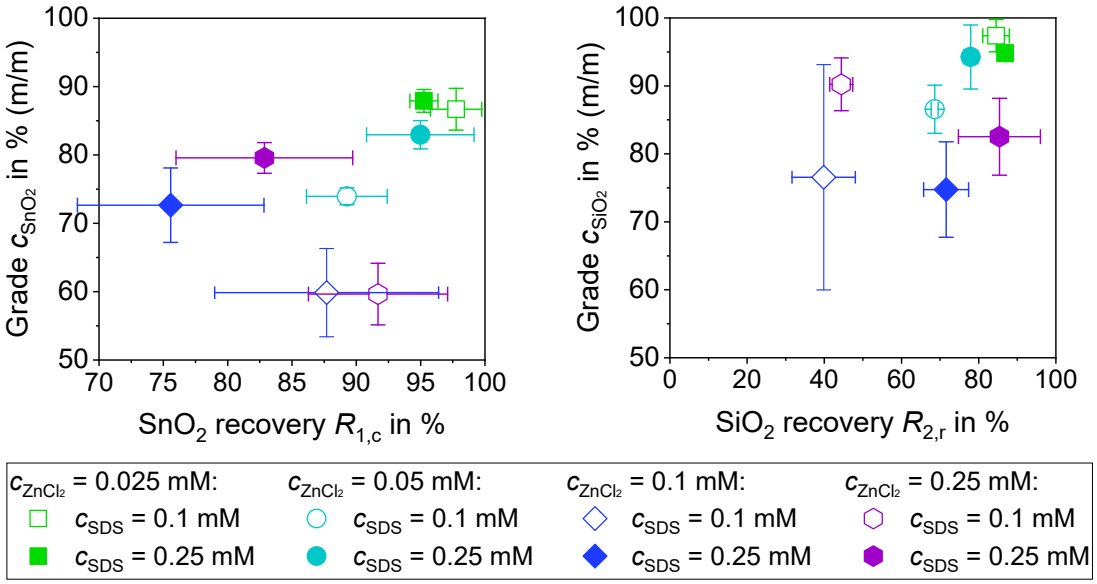


Figure 13. Grade-recovery diagrams from the liquid–liquid extraction experiments for the separation of the 1:1 mixture of SiO_2 and SnO_2 (0.5% (m/m)) for different $ZnCl_2$ and SDS concentrations at pH 6; left: results for the particles transferred to the oil phase, right: results for particles remaining in the aqueous phase. Data were already published in Heilmann et al. [38]. The data points show the average of three values and the bars represent the calculated standard deviation.

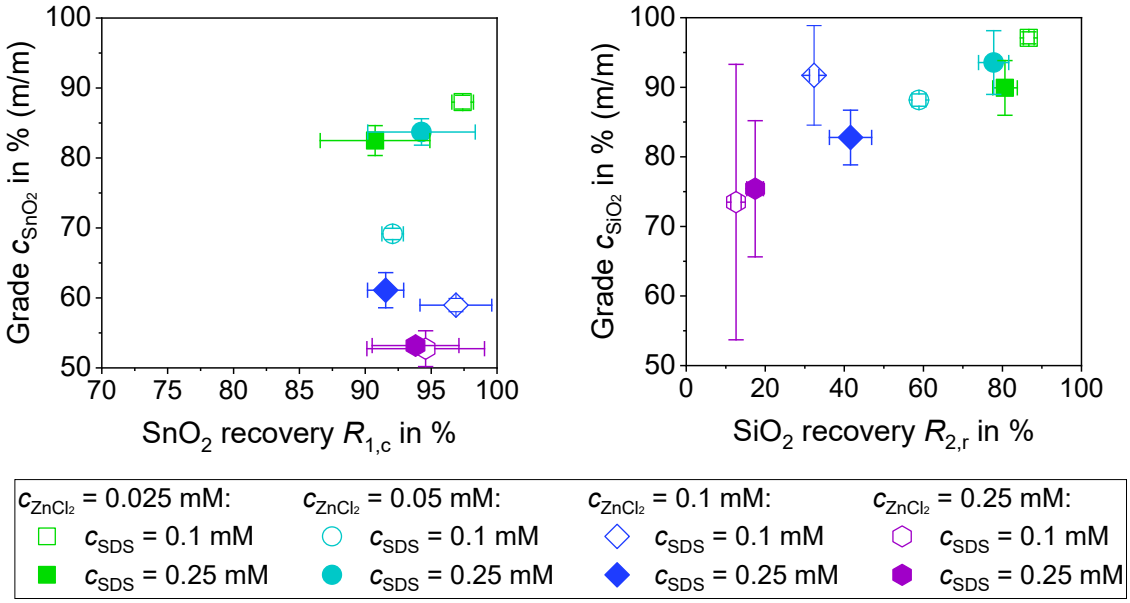


Figure 14. Grade-recovery diagrams from the liquid–liquid extraction experiments for the separation of the 1:1 mixture of SiO_2 and SnO_2 (0.5% (m/m)) for different salt and surfactant concentration at pH 8; left: results for the particles transferred to the oil phase, right: results for particles remained in the aqueous phase. Data were already published in Heilmann et al. [38]. The data points show the average of three values and the bars represent the calculated standard deviation.

Figure 13 shows the grade-recovery diagrams for the separation of a 1:1 mixture of SiO_2 and SnO_2 with a solids content of 0.5% (m/m).

It can be seen in Figure 13, left, high recoveries of over 70% were achieved for SnO_2 in the organic phase, with the grades varying significantly. For the two higher amounts of $ZnCl_2$ in the system, higher amounts of SDS cause the recovery to decrease as the mass recovery decreases, but at the same time the grade increases. This can be seen when comparing the data points at c_{ZnCl2} = 0.1 mM (blue dots) and 0.25 mM (violet dots) for both SDS concentrations. This is because the higher amount of SDS probably generates a surfactant bilayer around the SnO_2 particles. The negative head group of the SDS molecule then faces outwards. Electrostatic repulsion occurs with the negatively charged SiO_2 particles, preventing hetero-agglomeration, resulting in lower recovery but higher purity. At the lower SDS concentration, the quantity of particles passing into the organic phase increases with increasing $ZnCl_2$ concentration. This means that a high recovery is always achieved. However, the grade decreases with the increasing mass recovery. Even with the lower SDS concentration of 0.1 mM, the two higher $ZnCl_2$ concentrations c_{ZnCl2} = 0.1 mM (blue dots) and 0.25 mM (violet dots) perform less, resulting in higher recovery but lower purity. The best results were achieved with c_{ZnCl2} = 0.025 mM and c_{SDS} = 0.1 mM and 0.25 mM, both in terms of recovery and grade of SnO_2. The best results were obtained with a recovery of 95.3% and a grade of 87.9% (m/m) for 0.25 mM SDS and a recovery with 97.8% with a grade of 86.7% (m/m) for 0.1 mM SDS at pH 6 for the smallest $ZnCl_2$ concentration of 0.025 mM. The aqueous phase primarily contains SiO_2, with SiO_2 grades over 74% (m/m). The results differ, particularly with regard to the recoveries. The only values that differ significantly are the values at c_{ZnCl2} = 0.1 mM (blue dots), 0.25 mM (violet dots) and 0.1 mM SDS, as they achieve the lowest recovery around 38–40%. For the other parameters, the recoveries were above 68%. The lowest concentration of $ZnCl_2$ 0.025 mM gave the best purities of 84.5–86.9% (m/m) and recoveries of 94.8–97.4% for both SDS concentrations.

Experiments were also performed at pH 8 as shown in Figure 14. The adsorption of $ZnOH^+$ takes place on both particle surfaces of SiO_2 and SnO_2 as well as Zn^{2+} for SnO_2,

which provides an additional challenge to the separation, and thus the transfer of SnO_2 into the organic phase, while SiO_2 remains in the aqueous phase. In addition, the precipitation of the zinc ions and SDS ions also occur at this pH value, which affects the separation [12]. It is found that the mass recovery increases with increasing the zinc chloride concentration.

Even at pH 8, SnO_2 is transferred into the organic phase and the proportion of SiO_2, which is also transferred into the organic phase, increases with the increasing $ZnCl_2$ concentration, as can be seen from the decreasing grade of SnO_2.

Due to the adsorption on both particle surfaces, the zinc chloride ion concentration is reduced. Since precipitation also removes zinc ions and SDS from the solution, it does not seem possible to achieve a bilayer of SDS ions. The absence of repulsion leads to the hetero-agglomeration of the particles. For this reason, the purity decreases with increasing zinc chloride concentration. As the SnO_2 recovery is always above 90%, the results are very different in terms of purity. It is noticeable that the higher the zinc chloride concentration, the lower the purity of the organic phase. As with pH 6, it can be seen that the lowest zinc chloride concentration achieves the best separation results. The SiO_2 recovery depends significantly on the selected parameters. Similarly, to the organic phase, the purity of the aqueous phase decreases with increasing zinc chloride concentration. However, it is also obvious that the best separation is obtained at the lowest zinc chloride concentration. At pH 8, the best results were obtained with 0.025 mM $ZnCl_2$ and 0.1 mM SDS with a recovery of 97.4% and a grade of 88.0% (m/m) for the oil phase and a recovery of 86.7% and a grade of 97.1% (m/m) for the aqueous phase.

In summary, the most promising results were obtained at pH 6. Furthermore, the higher amount of surfactant was also beneficial for the separation of the materials. As shown in Table 7, a higher amount of $ZnCl_2$ of 0.125 mM for 0.375 g is required to cover the amount of SnO_2. However, it appears that agglomerates form and adhere to the emulsion droplets, so it is assumed that a monolayer of particles does not form. Therefore, at both pH 6 and pH 8, the lowest $ZnCl_2$ concentration results in the best separation results.

3.3.2. Separation of a 1:1 Mixture of SiO_2 and SnO_2 with $MgCl_2$ (0.5% (m/m))

Table 7 shows that the amount of $MgCl_2$ required to occupy the particles is significantly less than that for $ZnCl_2$. This is due to the different molar masses, as the ionic radii differ only slightly.

The results for the separation of a 1:1 mixture of SiO_2 and SnO_2 with different $MgCl_2$ concentrations at pH 6 are shown in Figure 15. The aim was to compare the efficiency of $ZnCl_2$ and $MgCl_2$ in terms of their selectivity. For this reason, the experiments were performed at pH 6, as at this pH value Mg^{2+} is only selectively adsorbed by SnO_2 and only low mass recoveries were obtained for SiO_2 during the phase transfer of the pure materials, as shown in Figure 12. The experiments show that SiO_2 and SnO_2 can be separated just as well as in the experiments with $ZnCl_2$ and similar trends can also be observed, which are explained in more detail below. Looking at the diagram of the results for the transfer to the organic phase (left) and the diagram of the results for the particles remaining in the aqueous phase (right), it can be seen that SnO_2 is transferred to the organic phase. In the organic phase, the amount of SiO_2 that passes over varies, as can be seen from the SnO_2 content.

The selectivity decreases with larger quantities of $MgCl_2$, as the mass recovery also increases. However, compared to the experiments with $ZnCl_2$ at pH 6, the mass recovery does not decrease during the experiments with the higher SDS concentration. It is therefore assumed that no SDS bilayer is formed, which would allow the repulsion of SiO_2 and SnO_2, although SDS is present in excess (Table 7). The hydrophobization of SiO_2 due to charge reversal with $MgCl_2$ and subsequent adsorption of SDS is excluded, as this was

only possible for small quantities during the phase transfer of pure SiO_2, as can be seen in Figure 12. Similarly, to pH 8 with $ZnCl_2$, the purity decreases with the increasing $MgCl_2$ concentration for both SDS concentrations. However, the recovery of SnO_2 in the organic phase remains the same. A trend that became apparent was that the results with the higher SDS concentrations showed quantitatively slightly higher recoveries and slightly higher purities. The best results for the particles passing into the organic phase were obtained with the parameters 0.025 mM $MgCl_2$ for 0.1 mM SDS. Looking at the results for the aqueous phase, the trend that emerged for the organic phase becomes more apparent. Although high SiO_2 grades of over 85% (m/m) were achieved in the aqueous phase, the results differ in terms of recovery. As the salt content increases, the recovery of SiO_2 decreases as more particles are transferred to the organic phase. The difference between the SDS concentrations for the respective $MgCl_2$ concentration is striking, as the results for the higher SDS concentration always show a higher recovery, except for 0.25 mM $MgCl_2$ where the recoveries are similar. The best purity and recoveries were achieved with the parameters 0.025 mM $MgCl_2$ for 0.1 mM and 0.25 mM SDS.

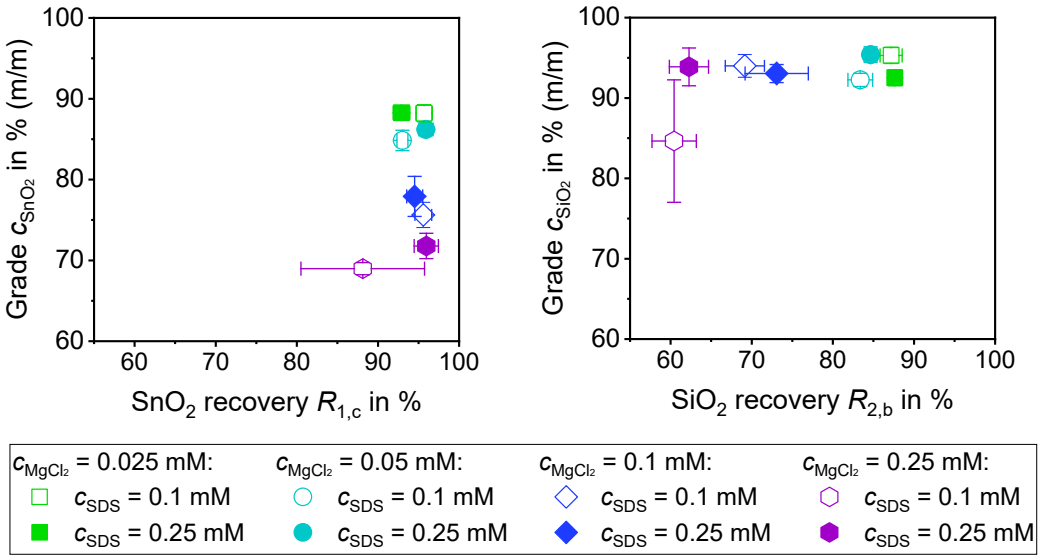


Figure 15. Grade-recovery diagrams from the liquid–liquid extraction experiments for the separation of the 1:1 mixture of SiO_2 and SnO_2 (0.5% (m/m)) for different $MgCl_2$ and SDS concentration at pH 6; left: results for the particles transferred to the oil phase, right: results for particles remained in the aqueous phase. The data points show the average of three values and the bars represent the calculated standard deviation.

Compared to $ZnCl_2$, a lower concentration of $MgCl_2$ is theoretically required to cover the SnO_2 particles. It is therefore also assumed that agglomerates attach to the emulsion droplets and that the lowest concentration of $MgCl_2$ is sufficient to achieve the best separation.

3.3.3. Separation of a 1:1 Mixture of SiO_2 and SnO_2 with $ZnCl_2$ (1% (m/m) and 2% (m/m))

The selectivity is checked by increasing the particle concentration. As seen in the previous experiments, the concentration of salt and SDS is important for the occupancy of the particles and therefore crucial for selectivity. Furthermore, the particle concentration could not be increased, as this would require a change in the setup, as the particles remaining in the aqueous phase would block the separation funnel. It would then no longer be possible to separate the phases. In addition, the organic phase eventually becomes saturated with particles so that no more particles can transfer.

Table 8 summarizes the quantities of ions required to occupy the particles at different particle concentrations. It is obvious that lower concentrations of $ZnCl_2$ are used than those required for the theoretical coverage of the particles. However, the theoretical coverage of the particles was calculated for a 1:1 mixture of SiO_2 and SnO_2, but the aim is to obtain only 50% SnO_2 in the mixture in the organic phase.

Table 8. Amounts of Zn^{2+} with their hydrolyzed species and SDS required for the occupancy of a 1:1 mixture of SiO_2 + SnO_2 for 1% (m/m) and 2% (m/m)).

Species	Required Concentration for the Individual Ions for a 1:1 Mixture of SiO_2 + SnO_2 in mM for:	
	1% (m/m)	2% (m/m)
Zn^{2+}	3.83	7.67
$Zn(OH)^+$	0.62	1.25
SDS	0.27	0.55

Comparing the calculated values for particle coverage and the actual concentration used, it is also noticeable that a low concentration of 0.025 mM to 0.25 mM $ZnCl_2$ was used. This means that there are too few ions in the solution to transfer all the particles of the 1:1 mixture of SiO_2 and SnO_2 into the organic phase. The same applies to the SDS concentration. However, only 0.25 mM is used, so there is a theoretical limitation as well, since not all particles can be hydrophobized.

Figure 16 shows the results for different salt concentrations for 0.25 mM SDS at pH 6 for higher particle concentrations, which should be compared with the results for a particle concentration of 0.5% (m/m) (Figure 13). The valuable product SnO_2, which has passed into the organic phase, is shown on the left and the grade of SiO_2, which has remained in the aqueous phase, is shown on the right.

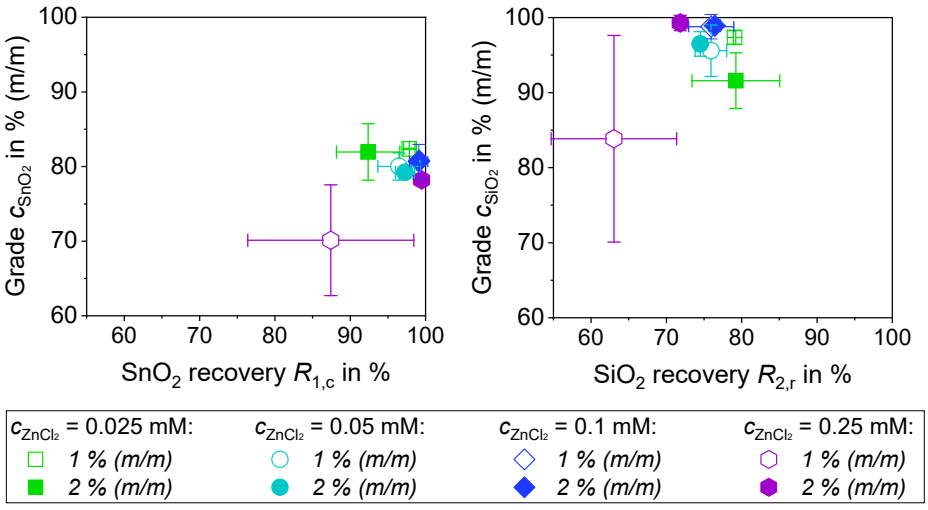


Figure 16. Grade-recovery diagrams from the liquid–liquid extraction experiments for the separation of the 1:1 mixture of SiO_2 and SnO_2 for 1% (m/m) and 2% (m/m) and different salt concentrations with 0.25 mM SDS at pH 6; left: results for the particles transferred to the oil phase, right: results for particles remained in the aqueous phase. The data points show the average of three values and the bars represent the calculated standard deviation.

The recovery of the particles that have passed into the organic phase remains high, above 80%. This means that in this experiment, SnO_2 was primarily transferred to the organic phase and the amount of SiO_2 varied. Depending on the salt concentration, more

or less SiO_2 is transferred to the organic phase, which is why the grade of SnO_2 in the oil phase decreases and the recovery of SiO_2 in the aqueous phase decreases. However, the purity decreases with increasing solid concentration for the $ZnCl_2$ concentration of c_{ZnCl2} = 0.025 mM. Compared to the results for the particles transferred to the organic phase at 0.5% (m/m), the grade of SnO_2 decreased from 97% to max. 83% with the same recovery for the best parameter of 0.025 mM $ZnCl_2$. This means that this concentration is no longer optimal for the process, as more SiO_2 is transferred to the organic phase. A similar grade but a better recovery $R_{1,c}$ of 100% was achieved for the $ZnCl_2$ concentration of 0.25 mM, which now gives the best separation result regarding the recovery. Theoretically, it was assumed that only SnO_2 would be transferred to the organic phase due to the lower mass recovery, as the aim was to adjust the salt and SDS concentration to preferentially hydrophobize only one particle system. Unfortunately, the amount of SDS could not suppress the hetero-agglomeration because the SDS concentration was too low, and the absence of the double layer means that no repulsion is possible, so low purity occurs.

A higher concentration of SDS could help to increase purity. Apart from the result with 0.25 mM $ZnCl_2$ for 1% (m/m), the other parameters gave very high recoveries of over 99%. The purity is between 75% (m/m) and 80% (m/m).

For the aqueous phase, SiO_2 recoveries between 70% and 80% were obtained. Except for the one value of 0.25 mM and 1%(m/m). As in the previous experiments, a very pure aqueous phase is obtained, since the recovery of SnO_2 in the organic phase is still high, the grade of SiO_2 in the aqueous phase is almost high and thus above 90% (m/m).

The fact that a transfer into the organic phase is possible at this low salt concentration and SDS concentration for the particles is due to the agglomeration of the particles. This is because less ions are required for charge reversal and hydrophobization. However, this would also mean that SnO_2 particles with different charges or with a low potential may be present and therefore agglomerate under these conditions.

3.3.4. Separation of Varied Mixing Ratios

The specific surface areas were only determined for pure substances and the 1:1 mixture of SiO_2 and SnO_2. For the values summarized in Table 9, the specific surface areas were calculated based on the determined values. Due to the higher specific surface area of SiO_2, the required quantities of ions and SDS increase with increasing SiO_2 content.

Table 9. Amounts of Zn^{2+} and the hydrolyzed species required and SDS for the occupancy of mixtures with different SnO_2 content for 0.5% (m/m).

Species	Required Concentration for the Individual Ions for Different SiO_2 + SnO_2 Mixtures in mM for:				
	80% SnO_2 + 20% SiO_2	**60% SnO_2 + 40% SiO_2**	**50% SnO_2 + 50% SiO_2**	**40% SnO_2 + 60% SiO_2**	**20% SnO_2 + 80% SiO_2**
Zn^{2+}	1.71	1.86	1.91	2.02	2.17
$Zn(OH)^+$	0.28	0.30	0.31	0.33	0.35
SDS	0.12	0.13	0.14	0.14	0.16

Furthermore, different mixture compositions were investigated for two different particle concentrations. For this study, the salt and surfactant concentrations were used, because they obtained the best results for the previously studied 1:1 mixture of SiO_2 and SnO_2 with 0.5% (m/m), which is also shown in Figure 17. For the separation c_{ZnCl2} = 0.025 mM and c_{SDS} = 0.25 mM were used at pH 6.

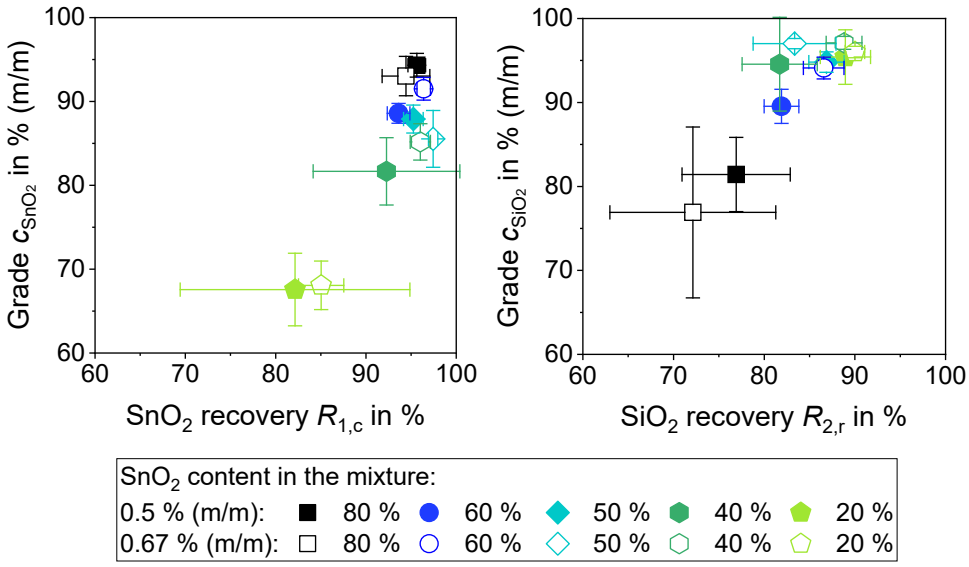


Figure 17. Grade-recovery diagrams from the liquid–liquid extraction experiments for the separation of different compositions of SiO_2 and SnO_2 mixtures for c_{ZnCl2} = 0.025 mM and c_{SDS} = 0.25 mM at pH 6; left: results for the particles transferred to the oil phase, right: results for particles remained in the aqueous phase. The data points show the average of three values and the bars represent the calculated standard deviation.

Figure 17 shows the results for the particles that have transferred to the organic phase on the left and the results for the particles remaining in the aqueous phase on the right. Since the valuable SnO_2 should be transferred to the organic phase, the left diagram is related to the grade and recovery of SnO_2. SiO_2 should remain in the aqueous phase, so the right diagram is based on the grade and recovery of SiO_2. It can be seen from both diagrams that SnO_2 is primarily transferred to the organic phase, as a high SnO_2 content was determined for the organic phase. A high SiO_2 content was also calculated for the aqueous phase for some data points, in particular for the mixtures with a higher SiO_2 content. The results for the transfer to the organic phase show that the mixtures with a higher SnO_2 content gave the better results, with a recovery of around 95% at a grade of 95% (m/m). With respect to the different mass concentrations, there are only minor deviations in terms of purity and recovery. The higher the SiO_2 content, the more the recovery and grade of the organic phase decrease. In conclusion, the less SnO_2 is present in the mixture, the higher is the SiO_2 content in the organic phase. Theoretically, due to the low zinc chloride concentration, only the SnO_2 should be addressed for a charge reversal. However, it appears that due to the different charges of SiO_2 and SnO_2 and the low potential difference at pH 6, agglomeration of SiO_2 and SnO_2 occurs, so that SiO_2 can also be transferred into the organic phase.

Only SDS is always present in sufficient quantities due to the concentration of 0.25 mM used, because the mixtures theoretically require only 0.11 to 0.16 mM SDS. For the mixture with the 80% SnO_2 content, the required SDS concentration is 0.11 mM. For this reason, bilayer formation is more pronounced in this mixture, resulting in stronger repulsion and thus better purity, as shown by the black dots in the left diagram. This means that the purification of mixtures with a high SiO_2 content is possible as well, but it will require a multi-stage separation to achieve the final grade. In this case, the $ZnCl_2$ concentration has to be adjusted for the higher SiO_2 content and thus reduced, as there is less SnO_2 on which the Zn species can adsorb. The situation is different for the particles remaining in the aqueous phase. The tests with the various mixtures have shown that there are only slight differences between the mixtures with a SiO_2 content of 50% or more in terms of purity and

recovery. The purity is above 94% (m/m) and the recovery is above 80%. The 1:1 mixture and the 1:4 mixtures for the lower mass concentration achieve the best results in terms of purity, and the 1:4 mixture for the lower mass concentration gives the best results in terms of recovery. The worst results were obtained for the mixture with the highest SnO_2 content, as significantly more SnO_2 remained in the aqueous phases with a recovery of 76.9% of and a grade of 81.4% (m/m) for the low mass concentration and with a recovery of 72.1% of and a grade of 76.9% (m/m) for the higher mass concentration.

4. Discussion

In order to separate the particles via liquid–liquid extraction, it is important to create a selective separation feature, where the wettability of the particles plays a crucial role. Due to the particle size distributions, shown in Figure 3, a size effect between the materials can be excluded, as they do not differ greatly from each other. As both metal oxides are negatively charged in aqueous solutions over a wide pH range, because the IEP of SiO_2 is below pH 3 and the IEP of SnO_2 is around pH 4, a hydrophobization of SiO_2 and SnO_2 by selective adsorption of a surfactant is not possible, as they do not adsorb on a specific surface. In order to create a selective separation property, positively charged hydrolyzed metal ions were used to adsorb onto the particle surface and form a bridge between the negatively charged particle surface and the negatively charged surfactant (SDS). The adsorption is recognized as a change in the sign of the zeta potential ζ and is referred to as charge reversal.

With the help of the specific surface area according to BET, the concentrations required to completely cover the particle surfaces and the particle surfaces in the mixtures could be calculated. Since SiO_2 SFP 20M has the highest S_{BET} of 10.05 ± 0.01 m^2/g, it requires more ions or SDS to be completely covered compared to SnO_2, which has an S_{BET} of 6.70 ± 0.06 m^2/g.

In the experiments with $AlCl_3$, it was shown, at various mass concentrations, that there is a correlation between the particle concentration and the concentration of $AlCl_3$ required for charge reversal. This indicates that the particles agglomerate during the measurement, which is probably due to the low potential when approaching the IEP. $ZnCl_2$ and $MgCl_2$ are suitable for the charge reversal of both materials, although the metal oxides differ in their adsorption behavior. SiO_2 requires a higher salt concentration than SnO_2 for the charge reversal due to the different IEPs. In addition, SiO_2 is selectively charged at a few pH values, while for SnO_2, a charge reversal is achieved over a wide pH range. The evidences from the previous experiments with the zeta potential could be confirmed with the liquid–liquid extraction experiments. SiO_2 shows selective behavior as a transfer into the organic phase is possible with $ZnCl_2$ at pH 8 and $MgCl_2$ at pH 8 to 10 with SDS. While SnO_2 particles transfer to the organic phase with $ZnCl_2$ at pH 4-pH 8 and with $MgCl_2$ at pH 4 to 10. In addition, the concentrations used for SnO_2 are not sufficient for SiO_2 to achieve a charge reversal of the particles, so hydrophobization with SDS was not possible. The experiments once again clearly showed how important the charge reversal of the particles is for the adsorption of SDS and thus for the hydrophobization of the particles.

For a selective separation, as a valuable substance, SnO_2 should be transferred to the organic phase, while SiO_2 remains in the aqueous phase. Due to different salt and surfactant concentrations, it was found that SnO_2 is transferred into the organic phase, so that enrichment occurs and that the amount of SiO_2 that is transferred depends on the pH-value, and the salt and surfactant concentration. The mass recovery in the oil phase at both pH values increased with the increasing $ZnCl_2$ concentration. Exclusively, at pH 6, no increase in mass recovery was observed at the higher SDS concentration. This can be explained by the adsorption of the SDS molecules, which have a bilayer structure at

higher concentrations. [19,52]. This is also confirmed by the fact that significantly more SDS was used at 0.25 mM than is theoretically required to form a monolayer (see Table 7). For separation, the bilayer structure of the SDS molecule is necessary to prevent the hetero-agglomeration of the materials. This is due to the repulsive effect of the negative head group of the DS^- molecule and the negatively charged SiO_2. At pH 8, no bilayer is formed by SDS. This is due to the fact that SDS can form a precipitate with the higher valent ions and thus the SDS and any excess Zn-ions are removed from the system [53]. The best results for pH 6 were obtained at the lowest $ZnCl_2$ concentration of 0.025 mM for the SDS concentrations of 0.1 mM and 0.25 mM. At pH 8, the best results were obtained at the lowest $ZnCl_2$ concentration of 0.025 mM with the lowest SDS concentration. As with $ZnCl_2$ separation, SnO_2 is mainly transferred to the organic phase during separation with $MgCl_2$, and the quantities of SiO_2 that are transferred vary. The SiO_2 content in the organic phase increases with the increasing $MgCl_2$ concentration. Furthermore, the bilayer structure of DS^- does not appear to be formed, as the values of the mass recovery do not change between the SDS concentrations. It is probably possible to separate the particles because the difference in concentration for the charge reversal of the particles is so far apart in both the electroacoustic and electrophoretic measurements. With the increasing mass concentration of the mixture, the selectivity decreases because more SiO_2 is transferred to the organic phase, as the SnO_2 grade in the organic phase decreases compared to the results of 0.5% (m/m). The $ZnCl_2$ concentration is probably still sufficient to achieve a charge reversal of the SnO_2, otherwise a higher grade of SnO_2 would have been obtained in the aqueous phase. Table 8 shows that the concentration of ions is theoretically too low at the different concentrations to achieve coverage of the particles. The fact that the $ZnCl_2$ is still sufficient to achieve a charge reversal of SnO_2 shows that it not only adsorbs the hydrolyzed species $Zn(OH)^+$, but also that Zn^{2+} can be adsorbed on SnO_2. Therefore, it is likely that the particles agglomerate at this concentration. Despite the agglomeration, the hydrophobicity seems to be sufficient to transfer the agglomerates into the organic phase. In addition, the amount of SDS is no longer sufficient to form a bilayer and, therefore, there is no negative charge that could have a repulsive effect on the negatively charged SiO_2 and thus prevent hetero-agglomeration. It would be useful to increase the SDS concentration in order to prevent hetero-agglomeration, so that higher purities can be achieved again. Furthermore, the selectivity was investigated with different mixture compositions. Due to the different BET surface areas, the lowest SDS concentration of 0.11 mM is required for the mixture with a 80% SnO_2 content. For this reason, the formation of the bilayer is more distinctive in this mixture, which leads to stronger repulsion, and thus, to better purity. For this reason, within the various mixtures, the higher the SnO_2 content in the initial mixture, the better the separation result, with respect to the organic phase. The more SiO_2 is added to the initial mixture, the more the selectivity of the separation process decreases, as the amount of SnO_2 is too low for the adsorption of the ions, thus favoring the transfer of the SiO_2 particles into the organic phase. In summary, it can be said that the separation of SiO_2 and SnO_2 is possible, and the separation performance depends on many parameters. If the separation method is to be applied to real cassiterite, the impurities contained therein must be taken into account, as these can have a considerable influence on the separation performance. In contrast to established methods such as flotation, it was shown that it is possible to separate SiO_2 and SnO_2 submicron particles. For industrial application, various parameters would have to be investigated further, and the batch tests transferred to a continuous separation column. It would then be necessary to check whether a higher level of force, for example, using a stirrer, is required for the particles to adhere to the emulsion droplets. The reversibility of the batch experiments would also have to be investigated, so that the organic phase can be used in the cycle. Furthermore, the method can also be

used for the separation of other metal oxide mixtures. For this, as with SiO_2 and SnO_2, it is necessary to find suitable salts.

5. Conclusions

The experiments showed that the adsorption of various salts leads to a charge reversal of the particles. By adding SDS as an anionic surfactant, selective pH hydrophobization can be achieved [12]. As SnO_2 and SiO_2 differ in their adsorption behavior, a separation feature is formed where SnO_2 is hydrophobized and can pass into the organic phase, while SiO_2 remains in the aqueous phase. The separation at pH 6 works significantly better at higher $ZnCl_2$ concentrations than at pH 8, especially in comparison to the results for the higher SDS concentrations. Significant differences are also observed at higher $ZnCl_2$ and the SDS concentration of 0.25 mM. This is due to the formation of a bilayer of DS^- at pH 6, which prevents hetero-agglomeration of the materials. Due to the precipitation of Zn-ions and SDS at pH 8, the formation of a DS^- bilayer cannot take place. The selective hydrophobization of SnO_2 allows the separation of the materials. The purity of the particles passing into the organic phase is strongly dependent on the mass concentration used, the salt and surfactant concentration and the chosen pH. Although the parameters for 0.025 mM $ZnCl_2$ or $MgCl_2$ and 0.1 mM and 0.25 mM SDS for pH 6 and for $ZnCl_2$ also at pH 8 achieved a very good separation for 0.5% (m/m), the selectivity was reduced when the mass concentration was increased. Differences in the separation with $MgCl_2$ and $ZnCl_2$ at pH 6 occurred only at higher salt concentrations. The batch tests in the separating funnel cannot be transferred 1:1 to industrial processes, as these run continuously. For this reason, it would be advisable to first transfer them to a separation column [39] and carry out parameter studies here. It is then necessary to check whether the particles stick to the emulsion droplets or whether a higher energy input is required. However, it is clearly shown that the separation of a SiO_2 and SnO_2 mixtures is possible. This means that this method can also be transferred to the separation of other metal oxide mixtures in the submicron range, as long as the IEP of the materials differs.

Author Contributions: C.H.: Writing—original draft preparation, methodology, investigation. L.D.: Supervision, writing—review and editing. M.R.: Supervision, writing—review and editing. U.A.P.: Supervision, funding acquisition, project administration, writing—review and editing. All authors have read and agreed to the published version of the manuscript.

Funding: The project (Project-Number: 382122817, GZ: PE 1160/26-2) in which the work was performed is funded by the German Research Foundation (DFG). The project was part of the SPP2045 "MehrDimPart".

Institutional Review Board Statement: Not applicable.

Informed Consent Statement: Not applicable.

Data Availability Statement: Data from the measurements can be requested from the corresponding authors.

Acknowledgments: The authors would like to thank Burkhart von Klitzing for providing the particles from Denka. Yvonne Volkmar is thanked for her experimental assistance with the measurements of the zeta potential with the Zetasizer Nano ZS and for the BET measurements. Annett Kästner is thanked for the particles size distributions and density measurements. The authors would like to thank Mina Asadijozani for her help with the XRF measurements and sample preparation. Peggy Knospe is thanked for the TEM images of the particles.

Conflicts of Interest: The authors declare no conflicts of interest.

References

1. Nguyen, A.; Schulze, H.J. *Colloidal Science of Flotation*, 1st ed.; Taylor & Francis Group: London, UK, 2004.
2. Zhang, L.; Khoso, S.A.; Tian, M.; Sun, W. Cassiterite recovery from a sulfide ore flotation tailing by combined gravity and flotation separations. *Physicochem. Probl. Miner. Process.* **2021**, *57*, 206–215. [CrossRef]
3. De, F.; Gontijo, C.; Fornasiero, D.; Ralston, J. The Limits of Fine and Coarse Particle Flotation. *Can. J. Chem. Eng.* **2007**, *85*, 739–747.
4. Gaudin, A.M.; Malozemoff, P. Recovery by Flotation of Mineral Particles of Colloidal Size. *J. Phys. Chem.* **1933**, *37*, 597–607. [CrossRef]
5. Gaudin, A.M.; Schuhmann, R., Jr.; Schlechten, A.W. Flotation Kinetics. II. The Effect of Size on the Behavior of Galena Particles. *J. Phys. Chem.* **1942**, *46*, 902–910. [CrossRef]
6. Rhein, F.; Zhai, O.; Schmid, E.; Nirschl, H. Multidimensional Separation by Magnetic Seeded Filtration: Experimental Studies. *Powders* **2023**, *2*, 37. [CrossRef]
7. Schubert, H. *Aufbereitung Fester Stoffe Band II: Sortierprozesse*, 4th ed.; Deutscher Verlag für Grundstoffindustrie: Stuttgart, Germany, 1996.
8. Englert, A.H.; Rodrigues, R.T.; Rubio, J. Dissolved air flotation (DAF) of fine quartz particles using an amine as collector. *Int. J. Miner. Process.* **2009**, *90*, 27–34. [CrossRef]
9. Crawford, R.; Ralston, J. The influence of particle size and contact angle in mineral flotation. *Int. J. Miner. Process.* **1988**, *23*, 1–24. [CrossRef]
10. Machunsky, S.; Grimm, P.; Schmid, H.-J.; Peuker, U.A. Liquid–liquid phase transfer of magnetite nanoparticles. *Colloids Surf. A Physicochem. Eng. Asp.* **2009**, *348*, 186–190. [CrossRef]
11. Yao, H.; Momozawa, O.; Hamatani, T.; Kimura, K. Stepwise Size-Selective Extraction of Carboxylate-Modified Gold Nanoparticles from an Aqueous Suspension into Toluene with Tetraoctylammonium Cations. *Chem. Mater.* **2001**, *13*, 4692–4697. [CrossRef]
12. Heilmann, C.; Ditscherlein, L.; Peuker, U.A. Influence of Hydrolyzed Metal Ions and Surfactants on the Phase Transfer of Al_2O_3, SiO_2, and SnO_2. *Langmuir* **2024**, *40*, 2543–2550. [CrossRef]
13. Machunsky, S.; Peuker, U.A. Liquid-Liquid Interfacial Transport of Nanoparticles. *Phys. Sep. Sci. Eng.* **2007**, *2007*, 034832. [CrossRef]
14. Erler, J.V.; Machunsky, S.; Franke, S.; Grimm, P.; Schmid, H.-J.; Peuker, U.A. Process Development of a Liquid-Liquid Phase Transfer of Colloidal Particles for Production of High-Quality Organosols. In *Colloid Process Engineering*; Kind, M., Peukert, W., Rehage, H., Schuchmann, H.P., Eds.; Springer International Publishing: Cham, Switzerland, 2015; pp. 371–398.
15. Leistner, T.; Embrechts, M.; Leißner, T.; Chehreh Chelgani, S.; Osbahr, I.; Möckel, R.; Peuker, U.A.; Rudolph, M. A study of the reprocessing of fine and ultrafine cassiterite from gravity tailing residues by using various flotation techniques. *Miner. Eng.* **2016**, *96–97*, 94–98. [CrossRef]
16. Zhou, Y.C.; Tong, X.; Wang, X.; Deng, Z.B.; Xie, X.; Xie, F. Beneficiation of Ultrafine Cassiterite from a Tin Tailings by Flotation. *Adv. Mater. Res.* **2013**, *616–618*, 643–648. [CrossRef]
17. Lan, Z.Y.; Zhou, Y.C.; Tong, X. Recovery of Fine Cassiterite from Tin Tailings Slime by Froth Flotation. *Adv. Mater. Res.* **2013**, *634–638*, 3478–3483. [CrossRef]
18. Leistner, T.; Türk, M.; Weber, A.; Weber, C.; Peuker, U.A. Selective Separation Using Fluid-Liquid Interfaces. *Mater. Sci. Forum* **2019**, *959*, 113–124. [CrossRef]
19. Fuerstenau, D.W.; Pradip. Zeta potentials in the flotation of oxide and silicate minerals. *Adv. Colloid Interface Sci.* **2005**, *114–115*, 9–26. [CrossRef]
20. Fuerstenau, D.W.; Colic, M. Self-association and reverse hemimicelle formation at solid-water interfaces in dilute surfactant solutions. *Colloids Surf. A Physicochem. Eng. Asp.* **1999**, *146*, 33–47. [CrossRef]
21. Feng, Q.; Wen, S.; Zhao, W.; Chen, Y. Effect of calcium ions on adsorption of sodium oleate onto cassiterite and quartz surfaces and implications for their flotation separation. *Sep. Purif. Technol.* **2018**, *200*, 300–306. [CrossRef]
22. Weber, C.; Peuker, U.A. On the Role of Hydrolyzable Metal Cations in the Adsorption of Anionic Surfactants on Negatively Charged Surfaces. *Front. Mater.* **2020**, *7*, 40. [CrossRef]
23. Tian, M.; Khoso, S.A.; Wang, L.; Sun, W.; Zhang, C.; Hu, Y. Selective separation behavior and its molecular mechanism of cassiterite from quartz using cupferron as a novel flotation collector with a lower dosage of Pb^{2+} ions. *Appl. Surf. Sci.* **2019**, *486*, 228–238. [CrossRef]
24. Feng, Q.; Wen, S.; Zhao, W.; Chen, H. Interaction mechanism of magnesium ions with cassiterite and quartz surfaces and its response to flotation separation. *Sep. Purif. Technol.* **2018**, *206*, 239–246. [CrossRef]
25. Kusaka, E.; Nakahiro, Y.; Wakamatsu, T. The role of zeta potentials of oil droplets and quartz particles during collectorless liquid-liquid extraction. *Int. J. Miner. Process.* **1994**, *41*, 257–269. [CrossRef]
26. Kusaka, E.; Kamata, Y.; Fukunaka, Y.; Nakahiro, Y. The role of hydrolyzed metal cations in the liquid-liquid extraction of ultrafine silica with dodecyl sulfate. *Miner. Eng.* **1997**, *10*, 155–162. [CrossRef]
27. Fuerstenau, M.C.; Rice, D.A.; Somasundaran, P.; Fuerstenau, D.W. Metal Ion Hydrolysis and Surface Charge in Beryl Flotation. *Trans IMM* **1964**, *73*, 381.

28. Ruan, Y.; Zhang, Z.; Luo, H.; Xiao, C.; Zhou, F.; Chi, R. Effects of Metal Ions on the Flotation of Apatite, Dolomite and Quartz. *Minerals* **2018**, *8*, 141. [CrossRef]
29. De Vos, W.M.; Lindhoud, S. Overcharging and charge inversion: Finding the correct explanation(s). *Adv. Colloid Interface Sci.* **2019**, *274*, 102040. [CrossRef]
30. Lyklema, J. Overcharging, charge reversal: Chemistry or physics? *Colloids Surf. A Physicochem. Eng. Asp.* **2006**, *291*, 3–12. [CrossRef]
31. Jiménez, M.L.; Delgado, Á.V.; Lyklema, J. Hydrolysis versus Ion Correlation Models in Electrokinetic Charge Inversion: Establishing Application Ranges. *Langmuir* **2012**, *28*, 6786–6793. [CrossRef]
32. Wernersson, E.; Kjellander, R.; Lyklema, J. Charge Inversion and Ion−Ion Correlation Effects at the Mercury/Aqueous $MgSO_4$ Interface: Toward the Solution of a Long-Standing Issue. *J. Phys. Chem. C* **2010**, *114*, 1849–1866. [CrossRef]
33. Matijević, E.; Couch, J.P.; Kerker, M. Detection Of Metal Ion Hydrolysis By Coagulation. IV. Zinc. *J. Phys. Chem.* **1962**, *66*, 111–114. [CrossRef]
34. Delgado, A.V.; González-Caballero, F.; Hunter, R.J.; Koopal, L.K.; Lyklema, J. Measurement and interpretation of electrokinetic phenomena. *J. Colloid Interface Sci.* **2007**, *309*, 194–224. [CrossRef] [PubMed]
35. Binks, B.P.; Rodrigues, J.A. Influence of surfactant structure on the double inversion of emulsions in the presence of nanoparticles. *Colloids Surf. A Physicochem. Eng. Asp.* **2009**, *345*, 195–201. [CrossRef]
36. Lyklema, H. *Fundamentals of Interface and Colloid Science*, Solid-liquid interfaces, 1st ed.; Academic Press: London, UK, 1995; Volume 2.
37. Somasundaran, P.; Healy, T.W.; Fuerstenau, D.W. Surfactant Adsorption at the Solid-Liquid Interface-Dependence of Mechanism on Chain Length. *J. Phys. Chem.* **1964**, *68*, 3562–3566. [CrossRef]
38. Heilmann, C.; Ditscherlein, L.; Asadijozani, M.; Rudolph, M.; Peuker, U.A. Separation of submicron SiO_2 and SnO_2 particles via liquid-liquid extraction using $ZnCl_2$ and SDS. *Sep. Purif. Technol.* **2025**, *366*, 132758. [CrossRef]
39. Leistner, T.; Müller, M.; Erler, J.V.; Rudolph, M.; Peuker, U.A. Selektive Trennung sehr feiner Partikelsysteme mittels Flüssig/Flüssig-Flotation. *Chem. Ing. Tech.* **2014**, *86*, 831–839. [CrossRef]
40. Israelachvili, J.N. Intermolecular and Surface Forces, 3rd ed.Academic Press: London, UK, 2011.
41. Atkins, P.W.; de Paula, J. *Kurzlehrbuch Physikalische Chemie*, 4th ed.; Wiley-VCH: Weinheim, Germany, 2008.
42. Atkins, P.W.; de Paula, J.; Keeler, J. *Atkins' Physical Chemistry*, 11th ed.; Oxford University Press: Oxford, UK, 2018.
43. Wiberg, N. *Lehrbuch der Anorganischen Chemie*; De Gruyter: Berlin, Germany, 2008.
44. Lide, D.R. *CRC Handbook of Chemistry and Physics*, 86th ed.; CRC Press: Boca Raton, FL, USA, 2005.
45. Shannon, R. Revised effective ionic radii and systematic studies of interatomic distances in halides and chalcogenides. *Acta Crystallogr. Sect. A* **1976**, *32*, 751–767. [CrossRef]
46. Müller, B.; ChemEQL—A Software for the Calculation of Chemical Equilibria. 2024, from the Department Surface Waters—Research and Management. Available online: https://www.eawag.ch/en/department/surf/projects/chemeql/ (accessed on 28 May 2025).
47. Kosmulski, M. Isoelectric points and points of zero charge of metal (hydr)oxides: 50 years after Parks' review. *Adv. Colloid Interface Sci.* **2016**, *238*, 1–61. [CrossRef]
48. Peuker, U.A.; Leißner, T. Solid–Solid Separation. In *Ullmann's Encyclopedia of Industrial Chemistry*; Wiley-VCH GmbH: Weinheim, Germany, 2023; pp. 1–20.
49. Küster, F.W.; Thiel, A. *Ruland, Rechentafeln für die Chemische Analytik*, 104th ed.; De Gruyter: Berlin, Germany, 1993.
50. Davies, S.H.R.; Morgan, J.J. Manganese (II) oxidation kinetics on metal oxide surfaces. *J. Colloid Interface Sci.* **1989**, *129*, 63–77. [CrossRef]
51. Kumar, K.Y.; Raj, T.N.V.; Archana, S.; Prasad, S.B.B.; Olivera, S.; Muralidhara, H.B. SnO_2 nanoparticles as effective adsorbents for the removal of cadmium and lead from aqueous solution: Adsorption mechanism and kinetic studies. *J. Water Process Eng.* **2016**, *13*, 44–52. [CrossRef]
52. Jańczuk, B.; Bruque, J.M.; González-Martín, M.L.; del Pozo, J.M. The surface free energy of fluorite in presence of sodium dodecyl sulfate. *Powder Technol.* **1994**, *80*, 127–131. [CrossRef]
53. Talens-Alesson, F.I. Behaviour of SDS micelles bound to mixtures of divalent and trivalent cations during ultrafiltration. *Colloids Surf. A Physicochem. Eng. Asp.* **2007**, *299*, 169–179. [CrossRef]

Disclaimer/Publisher's Note: The statements, opinions and data contained in all publications are solely those of the individual author(s) and contributor(s) and not of MDPI and/or the editor(s). MDPI and/or the editor(s) disclaim responsibility for any injury to people or property resulting from any ideas, methods, instructions or products referred to in the content.